Naval Research Laboratory

Washington, DC 20375-5000

(2)

NRL Memorandum Report 6522

AD-A212 706

Cavity Eigenmodes for the NIST/NRL Free Electron Laser

S. RIYOPOULOS* AND C.M. TANG

Plasma Theory Branch
Plasma Physics Division

**Science Applications Intl. Corp.*
McLean, VA 22102

September 5, 1989

Approved for public release; distribution unlimited.

SECURITY CLASSIFICATION OF THIS PAGE

REPORT DOCUMENTATION PAGE

Form Approved OMB No 0704-0188

1a REPORT SECURITY CLASSIFICATION UNCLASSIFIED	1b RESTRICTIVE MARKINGS
2a. SECURITY CLASSIFICATION AUTHORITY	3 DISTRIBUTION/AVAILABILITY OF REPORT Approved for public release; distribution unlimited.
2b. DECLASSIFICATION/DOWNGRADING SCHEDULE	
4. PERFORMING ORGANIZATION REPORT NUMBER(S) NRL Memorandum Report 6522	5 MONITORING ORGANIZATION REPORT NUMBER(S)
6a NAME OF PERFORMING ORGANIZATION Naval Research Laboratory 6b OFFICE SYMBOL (If applicable) Code 4790	7a. NAME OF MONITORING ORGANIZATION
6c. ADDRESS (City, State, and ZIP Code) Washington, DC 20375-5000	7b ADDRESS (City, State, and ZIP Code)
8a. NAME OF FUNDING/SPONSORING ORGANIZATION ONR 8b. OFFICE SYMBOL (If applicable)	9 PROCUREMENT INSTRUMENT IDENTIFICATION NUMBER
8c. ADDRESS (City, State, and ZIP Code) Arlington, VA 22217	10 SOURCE OF FUNDING NUMBERS PROGRAM ELEMENT NO: — PROJECT NO: 9M0214 TASK NO: — WORK UNIT ACCESSION NO: —

11. TITLE (Include Security Classification)
Cavity Eigenmodes for the NIST/NRL Free Electron Laser

12. PERSONAL AUTHOR(S)
Riyopoulos,* S. and Tang, C.M.

13a. TYPE OF REPORT	13b TIME COVERED	14. DATE OF REPORT (Year, Month, Day)	15 PAGE COUNT
Interim	FROM ________ TO ______	1989 September 5	44

16 SUPPLEMENTARY NOTATION
*Science Applications Intl. Corp., McLean, VA 22102

17 COSATI CODES			18 SUBJECT TERMS (Continue on reverse if necessary and identify by block number)
FIELD	GROUP	SUB-GROUP	Free electron lasers Resonator modes

19 ABSTRACT (Continue on reverse if necessary and identify by block number)

The cavity transfer matrix for the round trip of a light pulse in the optical resonator of the National Institute of Standards and Technology (NIST)/Naval Research Laboratory (NRL) Free Electron Laser (FEL) oscillator is derived. The cavity eigenmodes and the corresponding eigenvalues are obtained, using an expansion in Gaussian-Laguerre vacuum modes, by numerical diagonalization. The fractional power loss per eigenmode, caused by the finite sizes of the cavity mirrors and apertures are determined. It is found that the losses are very small over the entire wavelength regime of operation.

20 DISTRIBUTION/AVAILABILITY OF ABSTRACT ☒ UNCLASSIFIED/UNLIMITED ☐ SAME AS RPT ☐ DTIC USERS	21 ABSTRACT SECURITY CLASSIFICATION UNCLASSIFIED
22a NAME OF RESPONSIBLE INDIVIDUAL C.M. Tang	22b TELEPHONE (Include Area Code) (202) 767-4148 22c OFFICE SYMBOL Code 4790

DD Form 1473, JUN 86 — Previous editions are obsolete — SECURITY CLASSIFICATION OF THIS PAGE

S/N 0102-LF-014-6603

CONTENTS

CAVITY EIGENMODES FOR THE NIST/NRL FREE ELECTRON LASER

I. INTRODUCTION

The NIST(formerly NBS)/NRL FEL oscillator powered by a CW 185 MeV racetrack microtron is currently under construction[1-3]. A simplified model of the resonator cavity, consisting of the wiggler vacuum chamber and the two mirrors, is shown schematically in Fig. 1. Since stimulated emission takes place predominantly along the electron beam path, the vector potential of the radiation $\mathbf{A_R}$ is expressed in terms of the free space eigenmodes $\mathbf{A_R}(r) = A_{mp}(r)\ \exp(-i\omega t)\ \mathbf{e_{mp}}$ + cc of the paraxial wave equation[4], where $\mathbf{e}_{mp}$ is the polarization vector,

$$A_{mp}(r) = \frac{u_{mp}(r;W)}{\left(1 + \frac{z^2}{b^2}\right)^{1/2}}\ e^{ik\left(z + \frac{(x^2 + y^2)}{2R(z)}\right)}\ e^{i\zeta_{mp}(z)} \quad , \qquad (1)$$

$k = \omega/c$ is the wave number and ω is the frequency. In Eq. (1) the exponent $k[z + (x^2+y^2)/2R(z)]$ contains the phase variation on the wavelength scale $\lambda = 2\pi/k$, with spherical wavefronts of curvature $1/R(z) = z/(z^2 + b^2)$. The slow phase variation is given by $\zeta_{mp}(z) = (2m + p + 1)\tan^{-1}(z/b)$. The spot size of the radiation envelope is $W(z) = w\ (1 + z^2/b^2)^{1/2}$, where the distance z is measured from the position of the waist $w = (2b/k)^{1/2}$. The amplitude squared of the mode drops by 1/2 over a distance equal to the Rayleigh length b (also known as confocal parameter). Most of the radiation is confined within a cone parametrized by the dif[illegible]ion angle $\theta_d = W/z \simeq (\lambda/b\pi)^{1/2}$. For given wavelength λ, any two [illegible] the four parameters R, W, b, z determine a mode uniquely.

The amplitude profile $u_{mp}(r;W)$ contains the transverse spatial variation, equivalent to a small $k_\perp$, perpendicular to the z-direction. In cylindrical coordinates (r,θ,z), where $\tan\theta = x/y$, $r = (x^2+y^2)^{1/2}$, $u_{mp}(r,\theta;W)$ takes the form

Manuscript approved June 15, 1989.

$$u^{\pm}_{mp}(r,\theta;W) = a_{mp} \begin{pmatrix}\cos p\theta \\ \sin p\theta\end{pmatrix} \xi^{p/2} L^p_m(\xi)\, e^{-\frac{\xi}{2}} , \qquad \xi = \frac{2r^2}{W^2} , \qquad (2)$$

where + (-) signifies cosine (sine) poloidal dependence, $L^p_m(\xi)$ are the associated Laguerre polynomials and the normalizing factor a_{mp} = $[1/(1+\delta_{p0})\pi W^2]^{1/2}[m!/(m + p)!]^{-1/2}$.

In the presence of conducting walls the vacuum expansion (1) still provides the best representation, because (a) the chamber inner radius is much larger than the radiation spot size and (b) the transit time through the cavity and the length of the light pulse itself are too short tc allow multiple reflections on the walls and set up cavity eigenmodes. It can also be argued that the small fraction of the radiation reflected from the wall, acting as a perfect conductor for grazing incidence, is lost out of the resonator. The main effect of the chamber, therefore, comes from the two edge apertures, where the radiation spot size is maximum. The resonator is then modeled by a sequence of four optical elements, i.e., two apertures and two mirrors.

The radiation profile is altered after each encounter with an optical element. A pure incident mode $A_{mp}(r)$ will, in general, be partially transformed into different modes. This is caused by the finite size of the apertures, and, in addition, by spherical aberration and surface imperfections in case of the mirrors. Consider the incoming radiation to a given optical element as consisting of various modes (m,p) of the same curvature $R_i(z)$. Both incident and reflected radiation are expanded into eigenmodes, respectively as follows,

$$A^i(r_i) = \sum_{m,p} c^i_{mp} A_{mp}(r_i) \quad ,$$

$$A^o(r_o) = \sum_{n,q} c^o_{nq} A_{nq}(r_o) \quad . \tag{3}$$

The relation among the incident and reflected expansion coefficients c^i_{mp} and c^o_{pq} is written as

$$\mathbf{c}^o = \mathbf{R}\,\mathbf{c}^i \quad , \tag{4a}$$

or

$$c^o_{nq} = \sum_{m,p} R^{mp}_{nq}\, c^i_{mp} \quad , \tag{4b}$$

where R^{mp}_{nq} are the elements of the reflection matrix **R**.

The radiation profile at the end of the round trip inside the resonator will relate to the original profile through the resonator transfer matrix **M**,

$$\mathbf{M} = \mathbf{T}_2\,\mathbf{R}_2\,\mathbf{T}_2\,\mathbf{T}_1\,\mathbf{R}_1\,\mathbf{T}_1, \tag{5}$$

where $\mathbf{T}_i$ and $\mathbf{R}_i$ are the transmission matrices through the chamber apertures and the reflection matrices from the mirrors 1 and 2 respectively. The cavity eigenmodes $\mathbf{C}_j$ with eigenvalues ν_j are given by

$$\mathbf{M}\,\mathbf{C}_j = \nu_j\,\mathbf{C}_j \quad . \tag{6}$$

Since $\mathbf{M}$ is generally nondiagonal, the eigenmodes are mixtures of vacuum modes (1).

The electron beam is an active medium that changes the radiation profile during amplification in each passage. If G is the amplification matrix, then a steady state exists finally if the matrix equation

$$G\,\mathbf{M}\,C_s = g_s\,C_s \tag{7}$$

has solutions with $|g_s| = 1$. A steady state need not be an eigenmode of the empty resonator; this could happen only in the case of equal amplification g_a for each eigenmode, i.e., $G = g_a\,I$ where I is the identity matrix. In an FEL, a different gain is associated with each free space eigenmode. However, in cases when the off-diagonal elements of both G and $\mathbf{M}$ become vanishingly small, both the resonator modes and the final steady states approach the pure vacuum modes (1).

In this paper we first study the vacuum performance of the optical cavity. The detailed cavity mode structure in terms of vacuum modes and the associated eigenvalues are obtained by numerical diagonalization of the cavity matrix $\mathbf{M}$. The fractional power loss η_j per cavity mode per trip is found from the magnitude of the eigenvalue

$$\eta_j = 1 - |\nu_j|^2. \tag{8}$$

The profiles for the cavity modes are also obtained utilizing the expansion coefficients of C_j into the vacuum modes. We also examine the eigenmode structure of the combined gain-transfer matrix $G\,\mathbf{M}$ in cases of small gain.

II. TRANSFER MATRIX FOR A SINGLE OPTICAL ELEMENT

The reflection of Gaussian light beams from mirrors was studied in some detail in Ref. 5 for arbitrary angle of radiation incidence. In the limit of normal incidence considered here, the reflection matrix elements are given by the surface integrals

$$R_{nq}^{mp} = \iint_S d\theta_s \, dr_s \, r_s \frac{u_{mp}(r_s,\theta_s) \, u_{nq}(r_s,\theta_s)}{\left[1 + \dfrac{l_o^2}{b_o^2}\right]^{1/2}} \left[\frac{1 + \dfrac{z_s^2(r_s)}{b_o^2}}{1 + \dfrac{z_s^2(r_s)}{b_i^2}}\right]^{1/2} e^{i\Delta(r_s,\theta_s)}$$

$$\times \, e^{i\zeta_{nq}^i(z_s) - i\zeta_{mp}^o(z_s)} \, . \qquad (9)$$

The mirror surface S is spherical, expressed in the coordinate system (r_s,θ_s,z_s) with origin located at the mirror center, by

$$(z_s - R_m)^2 + r_s^2 = R_m^2 \, , \qquad (10)$$

where R_m is the mirror radius of curvature. Equation (10) is used to express z_s on the surface S in terms of r_s. The mirror boundary is given by

$$r_s^2 = \rho^2 \, , \qquad (11)$$

where ρ is the radius of the mirror cross-section.

The phase factor $\Delta(r_s,\theta_s)$, related to the optical path along the various rays connecting the incoming wavefront with its mirror image (reflected), must be approximately constant. Therefore, the curvature of the outgoing wavefront is related to the incoming and the mirror curvatures through

$$\frac{1}{R_o} = \frac{2}{R_m} - \frac{1}{R_i} . \tag{12}$$

The Rayleigh length b_o and the waist location l_o of the outgoing modes are yet to be determined.

It has been argued[5,6] that the amount of radiation scattered into other than the incoming modes, as well as that escaping behind the mirror, depends on three factors:

(a) Finite mirror size effects, of the order of

$$\exp\left(-\frac{\rho^2}{W_i^2}\right) , \tag{13}$$

where ρ is the mirror cross-section radius and W_i the incoming radiation spot size.

(b) Spherical aberration effects, of the order of

$$kW_i \left(\frac{W_i^2}{R_m^2}\right) , \tag{14}$$

coming from the phase term $\Delta(r_s,\theta_s)$ inside (9). Spherical aberration exists even when the mirror curvature matches the radiation curvature. It is caused by the fact that rays ending on a given spherical wavefront are not exactly perpendicular to it, since they originated from a finite size waist and not from a point at the center of curvature.

(c) Surface imperfections, for example, when the reflecting surface is not perfectly spherical.

Spherical aberration effects are usually less important. They will be addressed in future work, together with the potentially more important consequences caused by mirror deformations (buckling) due to heating.

Ignoring (b) and (c) amounts to setting $\Delta(r_s,\theta_s) = 0$ in (9). After substituting expression (2) for the eigenmodes u_{mp}, (9) becomes,

$$R_{nq}^{mp}(\mu,\alpha) = \delta_{pq}\, C_{nq}^{mp} \int_0^{2\mu} d\xi\, (\alpha^2\xi)^{\frac{q}{2}}\, \xi^{\frac{p}{2}}\, L_n^q(\alpha^2\xi)\, L_m^p(\xi)\, e^{-\frac{\alpha^2+1}{2}\xi} , \quad (15)$$

where $C_{nq}^{mp} = \alpha\, [m!n!/(m+p)!(n+q)!]^{1/2}$ and $\xi = 2r^2/W_i^2$. Since the surface S has rotational symmetry about the z-axis, it couples modes with the same poloidal θ dependence, $p = q$. The radial integration is carried out in Appendix A.

In general, the matrix R involves two independent parameters, the ratio of the mirror radius ρ to the radiation spot size squared, $\mu = (\rho/W_i)^2$, and the ratio of the incoming to outgoing spot sizes $\alpha = (W_i/W_o)$. Only the curvature of the reflected mode is set by the mirror, while the outgoing spot size is still a free parameter. This can be exploited by choosing the value W_o that maximizes the coefficient for the fundamental mode in the reflected radiation, i.e.,

$$\frac{\partial R_{00}^{00}}{\partial\alpha} = 0 . \quad (16)$$

Once W_o is selected, the exact location and size of the waist(s) for the reflected modes is determined by solving the system of equations

$$W_o = w_o \left[1 + \frac{l_o^2}{b_o^2}\right]^{1/2} , \qquad \frac{1}{R_o} = \frac{l_o}{l_o^2+b_o^2} . \quad (17)$$

The transmission matrix T through an aperture is given by

$$T = e^{i\pi} R , \quad (18)$$

where R is the reflection matrix for a plane mirror ($R_m = \infty$) of the same cross section ρ, while the curvature transformation is

$$\frac{1}{R_o} = \frac{1}{R_i} \; . \tag{19}$$

Aberration and surface imperfections do not affect transmission through apertures.

III. CAVITY EIGENMODES

We seek a class of cavity eigenmodes with the waist located in the middle of the vacuum chamber. Since the mode spot must remain unchanged $W_i = W_o$ during each transmission or reflection we elect $\alpha = 1$ inside the transfer matrix (5) for every optical element. The curvature R is not changed during transmission through an aperture. The mirror curvature, however, must match the incoming and outgoing radiation curvature, $R_i = R_o = R_m$ in (12). Therefore, for eigenmodes to exist, the equations

$$R_1 = \frac{L_1}{L_1^2 + b^2}, \qquad R_2 = \frac{L_2}{L_2^2 + b^2}, \tag{20}$$

must admit a positive solution for b. This is possible when

$$\left(1 - \frac{L}{R_1}\right)\left(1 - \frac{L}{R_2}\right) > 0, \qquad L = L_1 + L_2 . \tag{21}$$

Equation (21) is the optical stability condition for the cavity. Even with (21) satisfied the cavity modes will still decay slowly in time because of the finite size of the mirrors. According to (20), the Rayleigh length b for various wavelengths remains fixed for a given mirror configuration, while the waist w varies as $w = (b\lambda/\pi)^{1/2}$. The cross section of the electron beam is adjustable to give a good filling factor for the particular wavelength. The cross section of the chamber is oval and is approximated with a circular one of effective radius $\rho = (\rho_1\rho_2)^{1/2}$, where ρ_1 and ρ_2 are the major and minor aperture radii.

Because of the imposed axisymmetry, we look for cavity eigenmodes involving combinations of axisymmetric vacuum modes $p = q = 0$. The coefficients $c_j^{(n)}$ of the modes u_{n0} inside the j-th cavity mode $\mathbf{C}_j$

$$\mathbf{C}_j = [\, c_j^{(0)}, c_j^{(1)}, \ldots, c_j^{(n)}, \ldots \,], \tag{22}$$

and the corresponding eigenvalues ν_j are found by numerical diagonalization of the transfer matrix **M**, utilizing expressions (A3) with $\alpha = 1$ for each individual optical element inside (5). Eventually, the cavity matrix **M** depends on the spot to aperture size ratios for the four optical elements,

$$\mathbf{M}[\mu_1(\lambda),\ \mu_2(\lambda),\ \mu_3(\lambda),\ \mu_4(\lambda)]\ , \tag{23}$$

where in turn μ_i depends on the wavelength through

$$\mu_i(\lambda) = \left(\frac{\lambda}{\pi b}\right)^{1/2} \frac{\rho_i}{\left(1 + L_i^2/b^2\right)^{1/2}}\ . \tag{24}$$

Two general conclusions are made. First, it is found that, for radiation spot sizes smaller than about one third the aperture sizes, the dominant contribution in each cavity eigenmode comes from a single coefficient $c_j^{(n)}$. Cavity eigenmodes, in this case, approach pure vacuum modes, as expected from the smallness of the off-diagonal matrix elements in **M**. Second, if the eigenvalues are arranged according to magnitude, $|\nu_0| > |\nu_1| > \ldots\ |\nu_j| > |\nu_{j+1}|\ ..$, the largest eigenvalue corresponds to the eigenmode closest to the fundamental vacuum mode u_{00}, i.e., the eigenmode with $|c_0^{(0)}| \simeq 1$. The next largest eigenvalue corresponds to the eigenmode closest to the first radial vacuum mode, i.e., with $|c_1^{(1)}| \simeq 1$, and so on. This is expected as the rms spot size for the n-th radial mode $u_{n0}(r;W)$ increases with n as $(n+1)^{1/2}W$.

The NIST/NRL oscillator has been designed for eigenmodes of Rayleigh length equal to half the vacuum chamber length. Two different arrangements, one with full wiggler and one with half length wiggler will be used for the wavelength regimes of 0.2μm to 2μm and 2μm to 10μm respectively. The design parameters are $b = L_w/2 = 107.5$cm, $L_1 = 521$cm,

L_2 = 386cm, R_1 = 543cm, R_2 = 417cm, $\rho_1 = \rho_2$ = 2.54cm for the half wiggler and b = $L_w/2$ = 196cm, L_1 = 431cm, L_2 = 477cm, R_1 = 521cm, R_2 = 559cm for the full wiggler.

The fractional power loss $\eta_j = 1 - |\nu_j|^2$ for the first 5 cavity eigenmodes of the half wiggler arrangement is plotted in Fig. 2 as a function of the wavelength λ. Through the planned regime of operation the loss for the fundamental cavity mode never exceeds 1%. The loss factor for the next two modes is also very small, so that the mode selection is going to be determined by the differences in the radiation gain for each mode. In Fig. 3(a) we plot the expansion coefficients $c_n^{(0)}$ of the fundamental cavity mode C_0 into the vacuum modes u_{n0}. It shows that the cavity mode profile is very close to a pure u_{00} vacuum mode, with other modes contributing less than 1%. The expansion coefficients for the second and third cavity modes are shown in Figs. 3(b) and 3(c) respectively. If the complete expansion coefficients are written as

$$c_j^{(n)} = |c_j^{(n)}| \exp(i\chi_{jn}) ,$$

then the complex amplitude for the j-th eigenmode C_j is given by

$$A_j(r) = |A_j(r)|\, e^{i\Phi_j(r)} ,$$

where

$$|A_j(r)| = \left[Ar_j^{\,2} + Ai_j^{\,2} \right]^{1/2}, \qquad \Phi_j(r) = \tan^{-1}\left(Ar_j \,/\, Ai_j \right) ,$$

$$Ar_j = \sum_n u_{n0}(r)\, |c_j^{(n)}| \cos \chi_{jn} , \qquad Ai_j = \sum_n u_{n0}(r)\, |c_j^{(n)}| \sin \chi_{jn} .$$

The resulting amplitude profiles for the first three modes at $z = 0$ are shown in Fig. 4 for $\lambda = 2\mu m$ and $\lambda = 10\mu m$. In Fig. 5(a) we show the power fraction η_j for the first four cavity modes of Rayleigh length $b = L_w/6$. The vacuum expansion coefficients $c_0^{(n)}$ for the fundamental cavity mode are shown in Fig. 5(b) against the wavelength λ. The transverse amplitude profiles for the first three modes at $\lambda = 2.2\mu m$ and $\lambda = 10\mu m$ respectively in Figs. 5(c) and 5(d), show considerable departure from vacuum modes.

The cavity eigenmodes for the full wiggler arrangement are extremely close to vacuum modes and the fractional power losses for the first five of them are below 10^{-3} over the frequency regime from $0.5\mu m$ to $2\mu m$. This is caused by the combination of a longer Rayleigh length with a spot size that gets smaller with shorter wavelength.

In case of small gain we can include the effect of the electron beam on the cavity eigenmodes by introducing the amplitude gain matrix **G**. In the linear regime the cross-coupling among various transverse modes is unimportant and **G** is diagonal, given by

$$G_{mn} = g(\lambda)\ f_n\ \delta_{mn}, \tag{25a}$$

where

$$g(\lambda) = 0.5\ F_1^2\ \frac{\pi^2}{\sigma_R}\ \frac{I}{I_A}\ \frac{\lambda_w^2}{\gamma_o^2}\ K^2\ N^3 \tag{25b}$$

is the amplitude gain for the fundamental vacuum mode. In Eqs. (25) N is the number of wiggler periods, γ_o is the initial relativistic factor, $\sigma_R = \pi w^2$ is the radiation cross section at the waist, $I_A = 17\times10^3$ A, I is the current in amperes, $K = |e|B_w\lambda_w/2\pi mc^2$ is the wiggler parameter, B_w is the rms magnetic field of the wiggler, λ_w is the wiggler wavelength, related to the radiation wavelength λ by $\lambda_w = 2\gamma^2\lambda/(1+K^2)$, $F_1 = J_o(b)-J_1(b)$ with b $= K^2/2(1+K^2)$ and f_n is the normalized (to the fundamental) filling factor

$$f_n = \int_0^\infty dr\ r\ j(r)\ u_{n0}(r) \Big/ \int_0^\infty dr\ r\ j(r)\ u_{00}(r)\ , \tag{26}$$

with the parabolic current profile given by $j(r) = j_o\ (1 - r^2/\rho_b^{\ 2})$ for $r \leq \rho_b$, $j(r) = 0$ for $r > \rho_b$, ρ_b being the beam radius. The round trip gain for the j-th beam-cavity eigenmode is given by

$$g_j = [\ 1 + g(\lambda)\ ]\ \tilde{\nu}_j, \tag{27}$$

where $\tilde{\nu}_j$ is the eigenvalue for the eigenmode $\tilde{C}_j$ of the combined gain-transfer matrix

$$M_g = G\ M\ . \tag{28}$$

The fractional power loss $\tilde{\eta}_j = 1 - |\tilde{\nu}_j|^2$ for the first five eigenmodes is shown in Fig. 6 as a function of the wavelength, while the expansion coefficients of the fundamental eigenmode in terms of vacuum modes are shown in Figs. 7(a)-7(c). The losses for the higher eigenmodes $j > 0$ are now considerably higher than the fundamental mode (compare Figs. 2 and 6), thusly, mode selection among transverse modes occurs through amplification of the radiation, because of the differences in the filling factor f_n. The transverse amplitude profiles at $\lambda = 2.2\ \mu m$ and $\lambda = 10\ \mu m$ appear in Figs. 8(a) and 8(b).

ACKNOWLEDGMENT

This work supported by ONR Contract No. N00014-87-f-0066 through National Institute of Standards and Technology (NIST).

REFERENCES

1. S. Penner et al., IEEE Trans. Nucl. Sci. NS-32 (5), 2669 (1985).
2. C. M. Tang, P. Sprangle, S. Penner and X. Maruyama, J. Appl. Phys. 63, 5233 (1988).
3. S. Penner et al., Nucl. Instr. and Methods Phys. Res., A272, 73 (1988).
4. See, for example, H. A. Haus in Waves and Fields in Optoelectronics, (Prentice Hall, New Jersey, 1984), p. 180, and references therein.
5. S. Riyopoulos, C. M. Tang and P. Sprangle, IEEE J. Quant. Electronics 25, 803 (1989).
6. S. Riyopoulos, P. Sprangle, C. M. Targ and A. Ting, Nucl. Instr. and Methods in Phys. Res. A272, 543 (1988).

APPENDIX A. Computation of the Reflection Matrix Element

The associated Laguerre polynomials are given by

$$L_m^p(\xi) = \sum_{k=0}^{m} (-1)^k \frac{(m+p)!}{k!(m-k)!(p+k)!} \xi^k . \tag{A1}$$

Substituting (A1) inside (15) and integrating by factors, using

$$\int d\xi \, \xi^n \, e^{-\xi} = - e^{-\xi} \left[\sum_{k=0}^{m} \frac{m!}{(m-k)!} \xi^{m-k} \right] , \tag{A2}$$

one obtains

$$R_{nq}^{mp}(\mu,\alpha) = \delta_{pq} \left[m!n!(m+p)!(n+q)! \right]^{1/2} \frac{\alpha^{p+1}}{\left(\frac{1+\alpha^2}{2}\right)^{p+1}} \sum_{k=0}^{m} \sum_{l=0}^{n} \alpha^{2k} \left(\frac{2}{\alpha^2+1}\right)^{k+l}$$

$$\frac{(-1)^{k+l}(k+l+p)!}{k!l!(m-k)!(n-l)!(p+k)!(p+l)!} \left(1 - e^{-(\alpha^2+1)\mu} \sum_{i=0}^{k+l+p} (2\mu m)^{k+l+p-i} \frac{\left(\frac{\alpha^2+1}{2}\right)^{p-i}}{(k+l+p-1)!} \right) . \tag{A3}$$

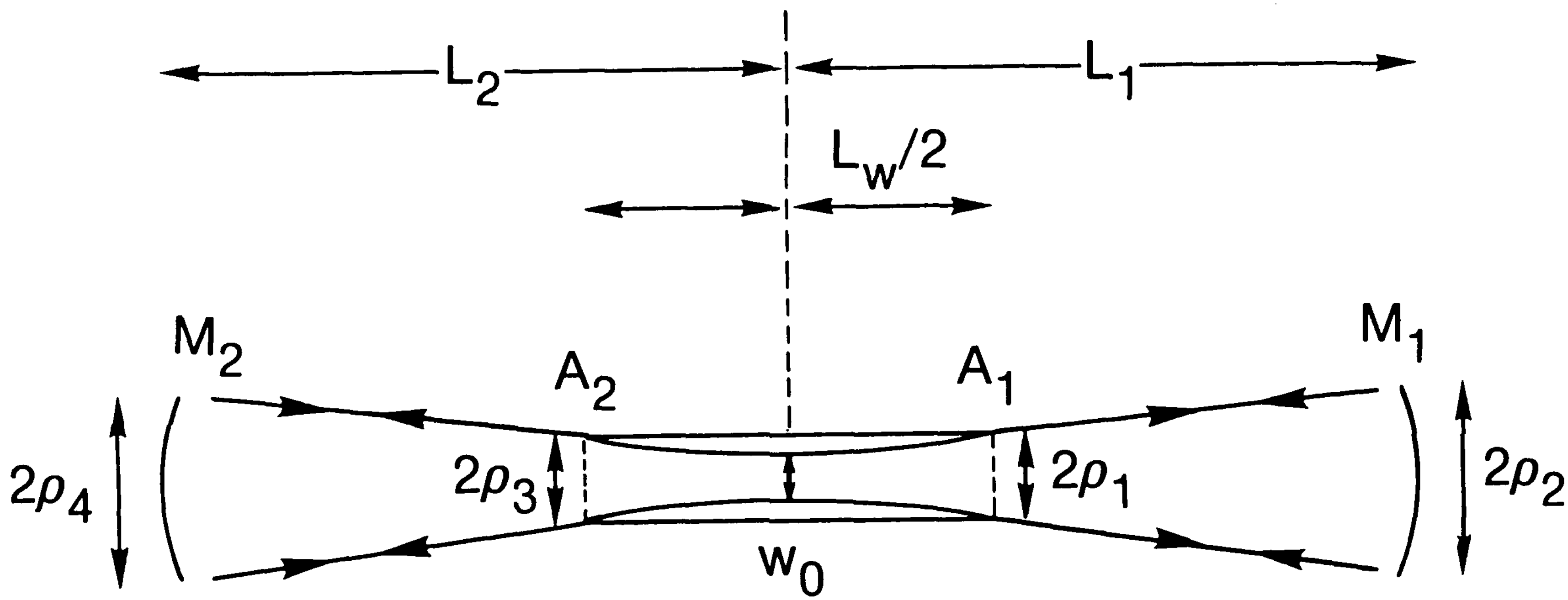

Fig. 1 — Schematic illustration of the NIST/NRL optical cavity.

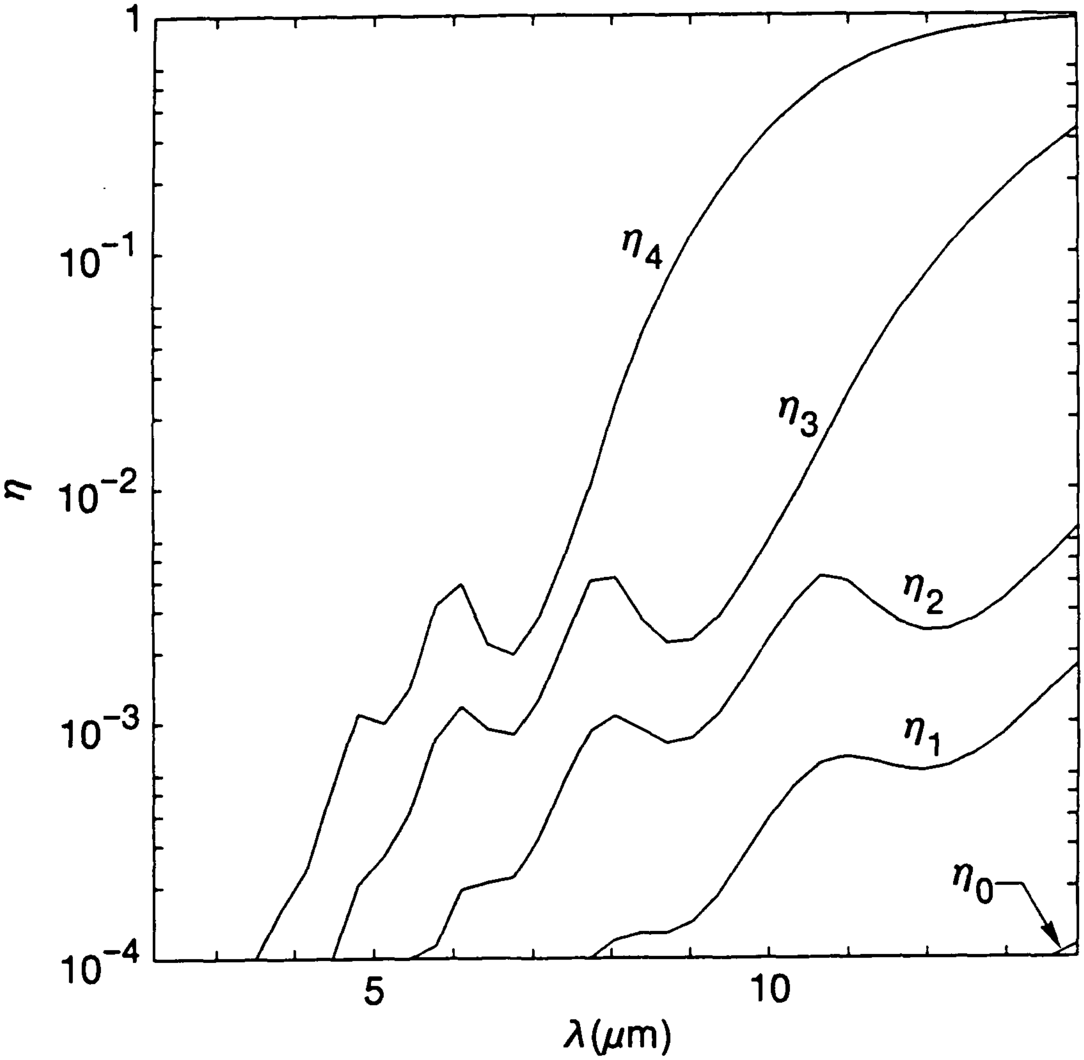

Fig. 2 — Fractional per round trip power loss versus wavelength for the first five resonator eigenmodes in vacuum. The Rayleigh length b is half the wiggler length. The cavity parameters for the half wiggler arrangement are L_1 = 521cm, L_2 = 386cm, R_1 = 543cm, R_2 = 417cm and $\rho_1 = \rho_2$ = 2.54cm.

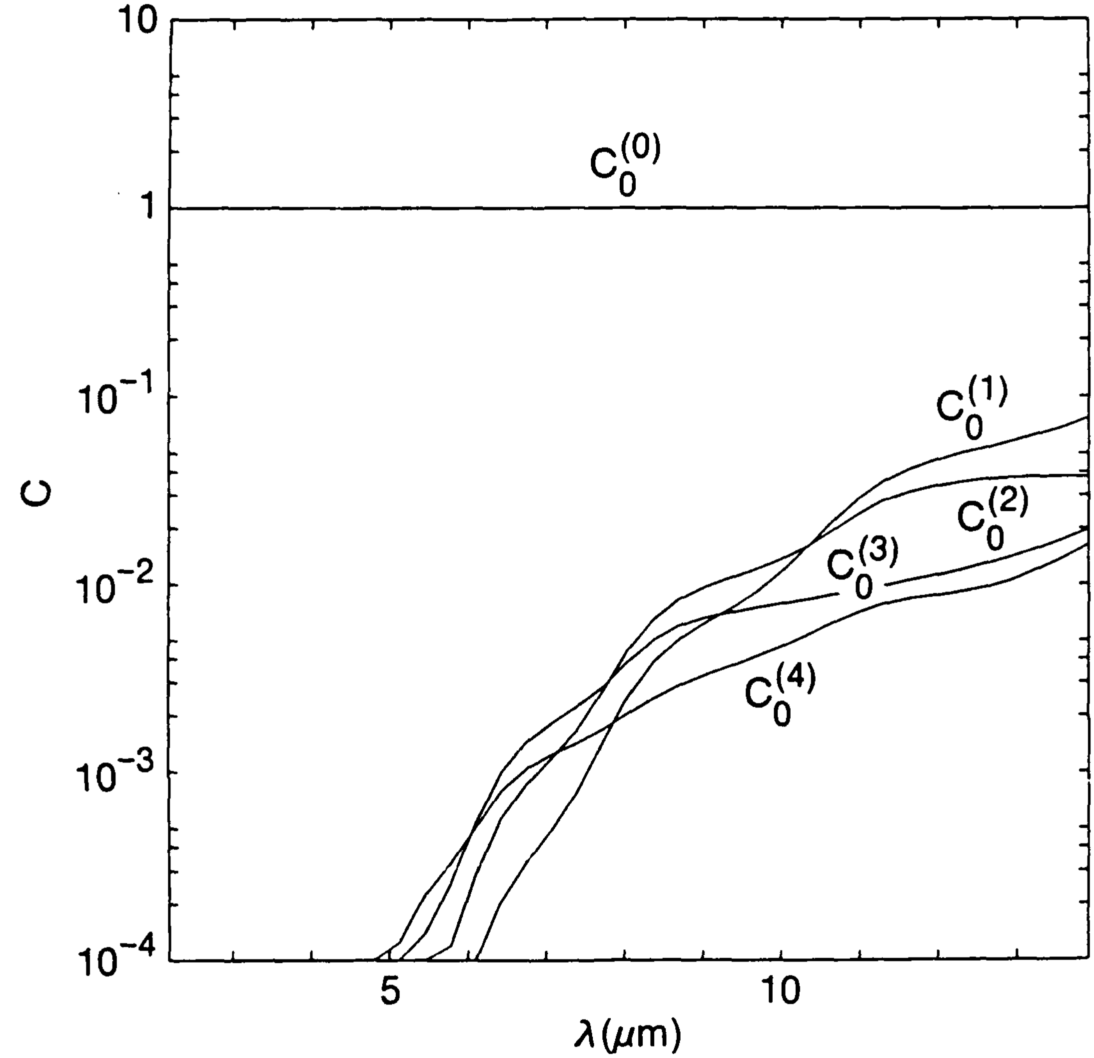

Fig. 3a — Expansion coefficients into vacuum modes for the fundamental cavity eigenmode versus wavelength.

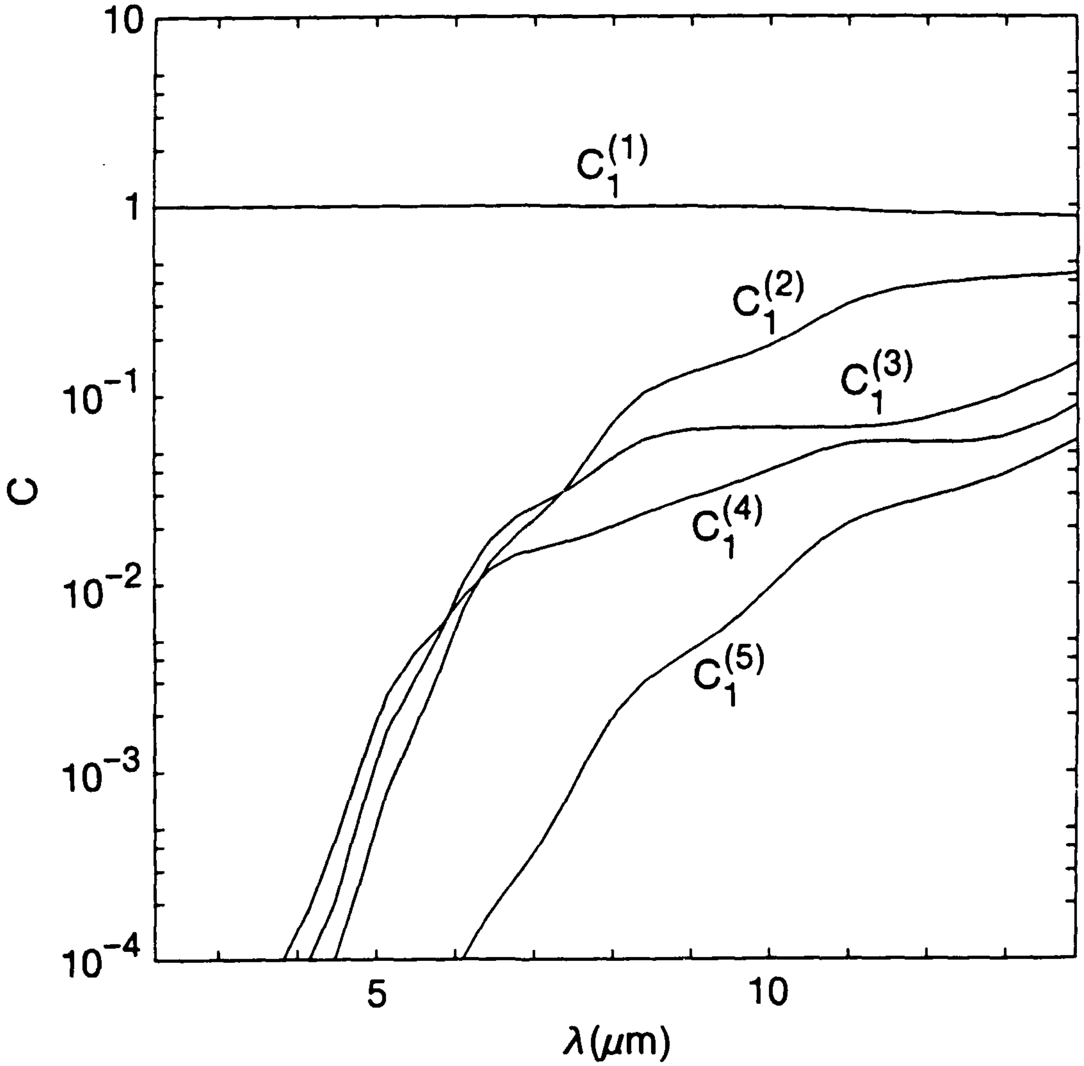

Fig. 3b — Expansion coefficients into vacuum modes for the first cavity eigenmode versus wavelength.

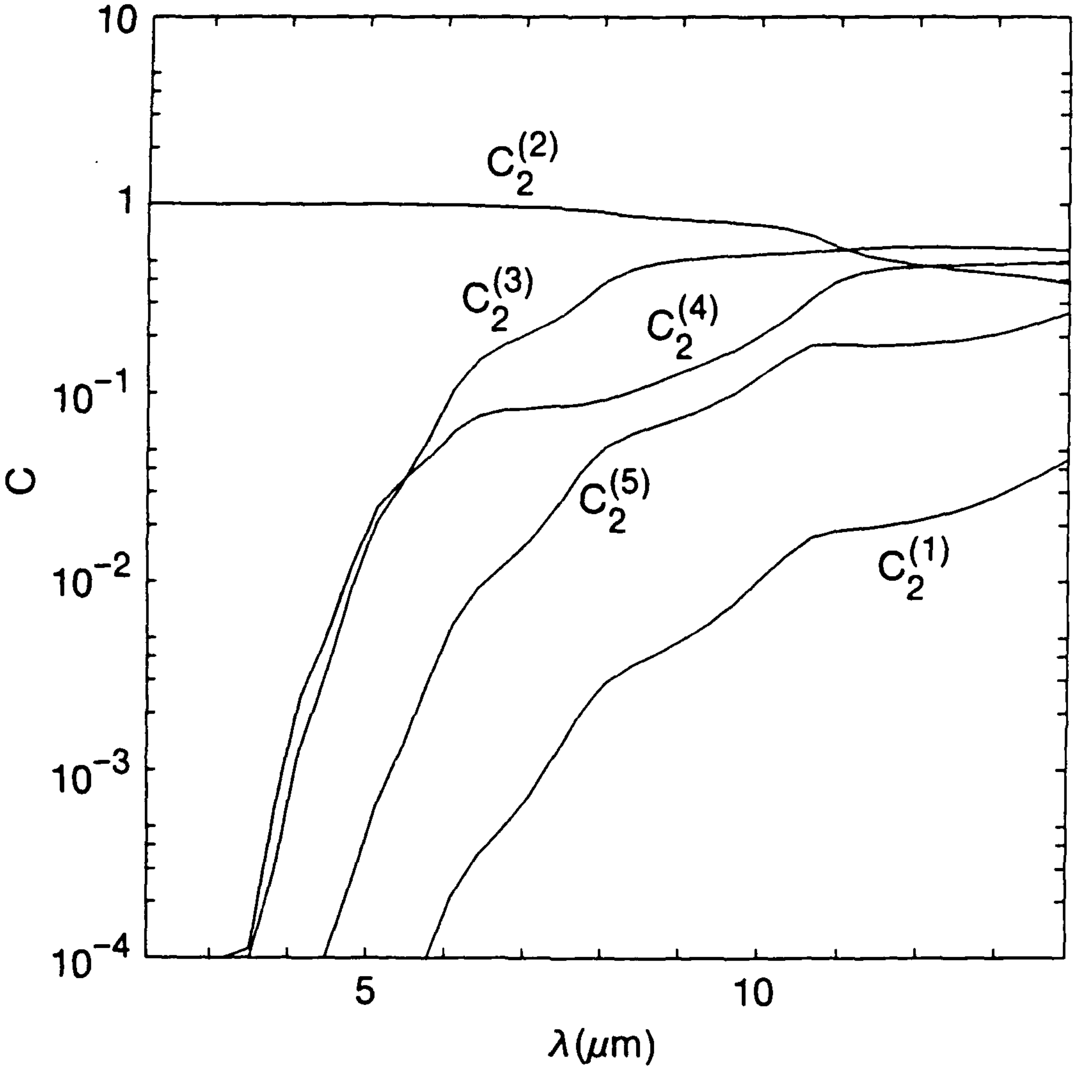

Fig. 3c — Expansion coefficients into vacuum modes for the second cavity eigenmode versus wavelength.

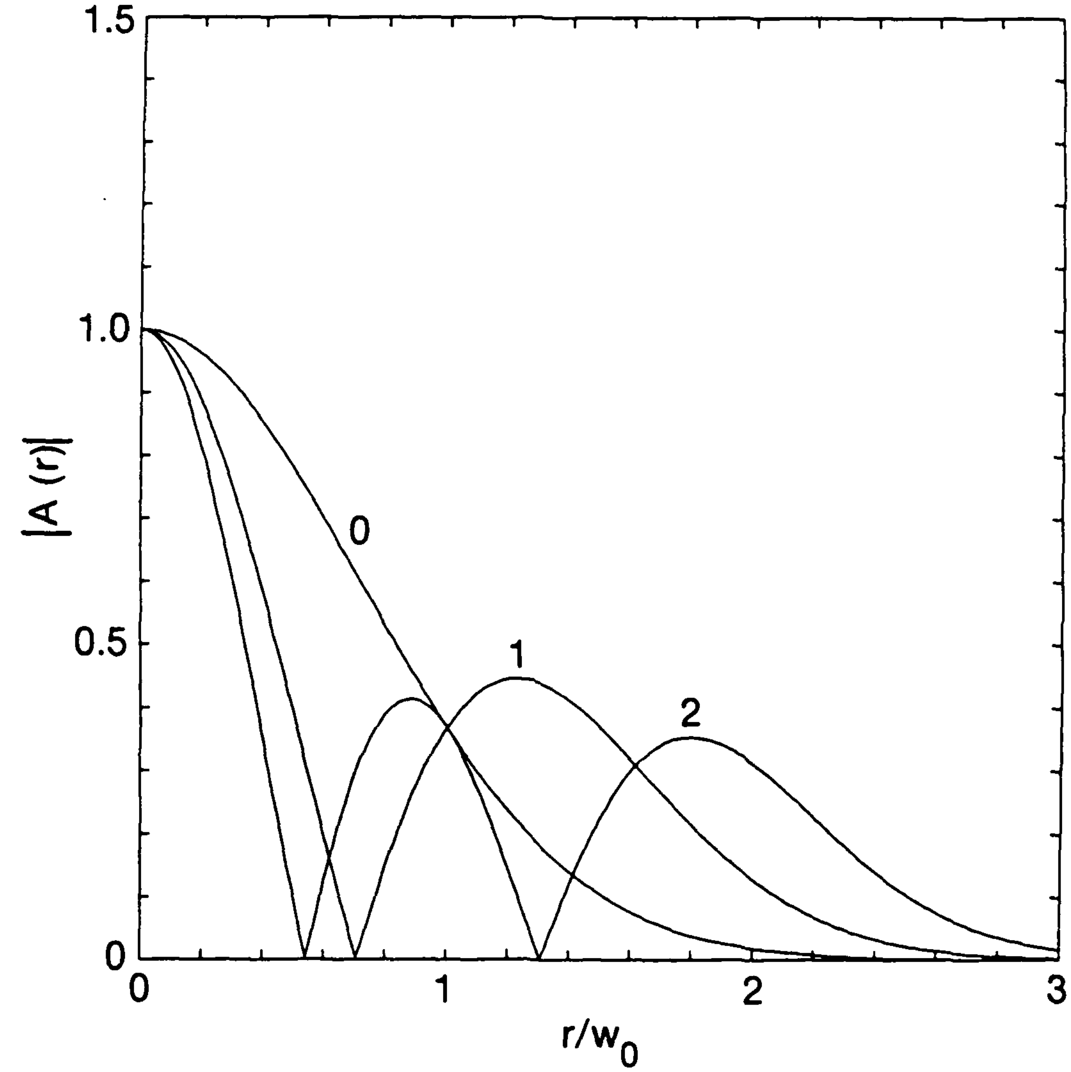

Fig. 4a — The transverse amplitude profiles $|A(r)|$ for the first three axisymmetric cavity modes for wavelength $\lambda = 2.2 \mu m$.

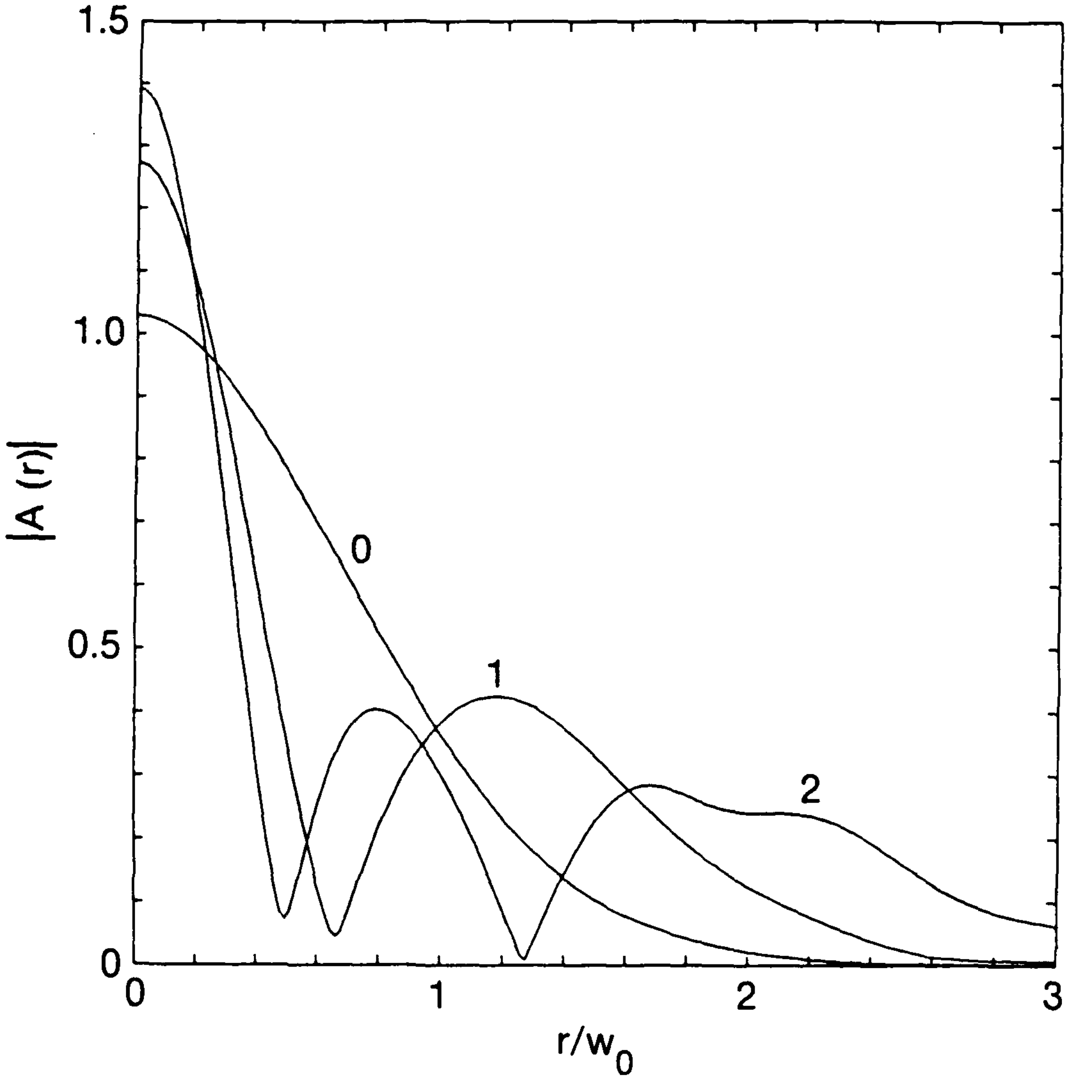

Fig. 4b — The transverse amplitude profiles $|A(r)|$ for the first three axisymmetric cavity modes for wavelength $\lambda = 10.0\mu$.

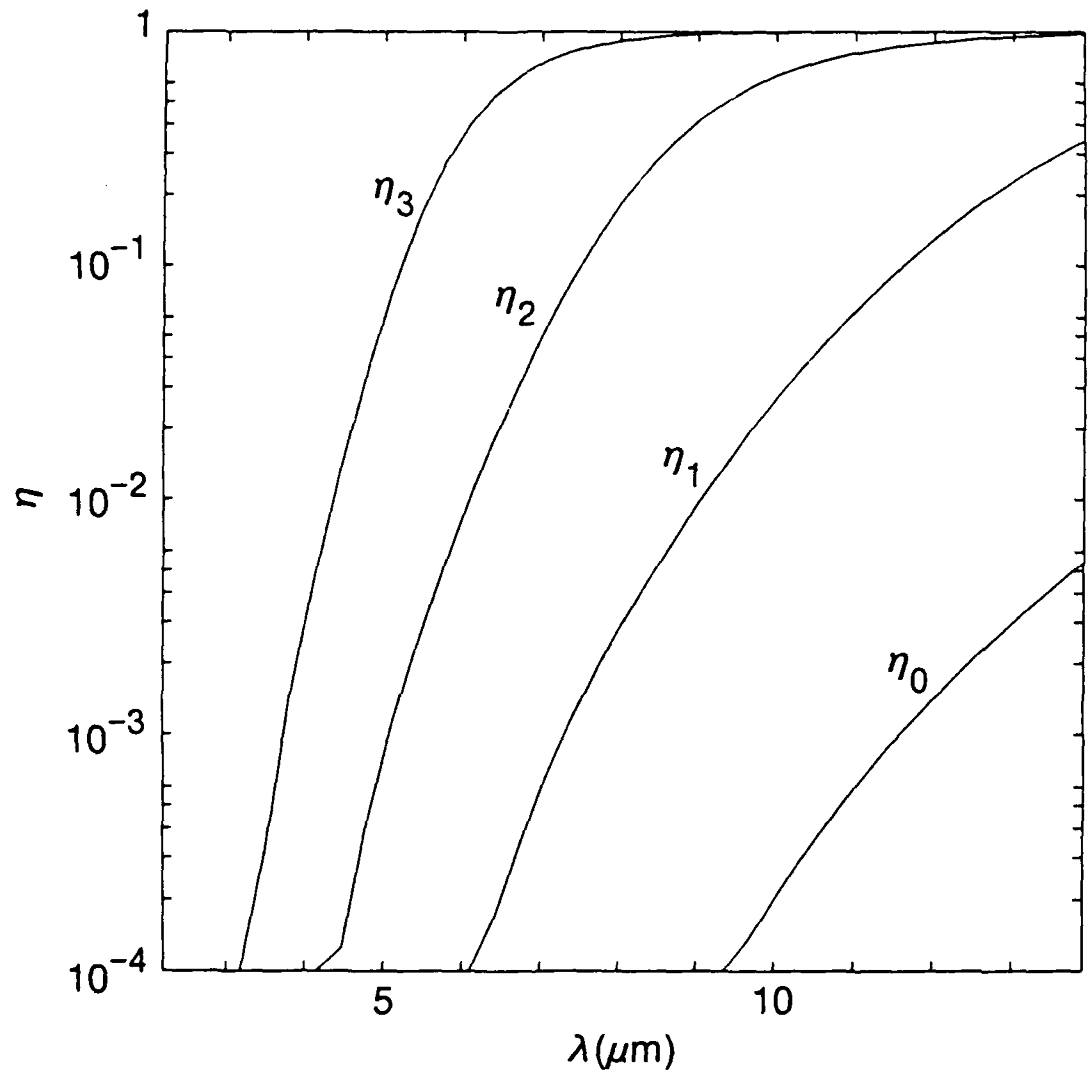

Fig. 5a — Plots of fractional round trip losses η for the first four eigenmodes versus wavelength where the fundamental cavity mode structure has Rayleigh length of $b = L_w/6$ and corresponding mirror curvatures of $R_1 = 523$cm and $R_2 = 389$cm.

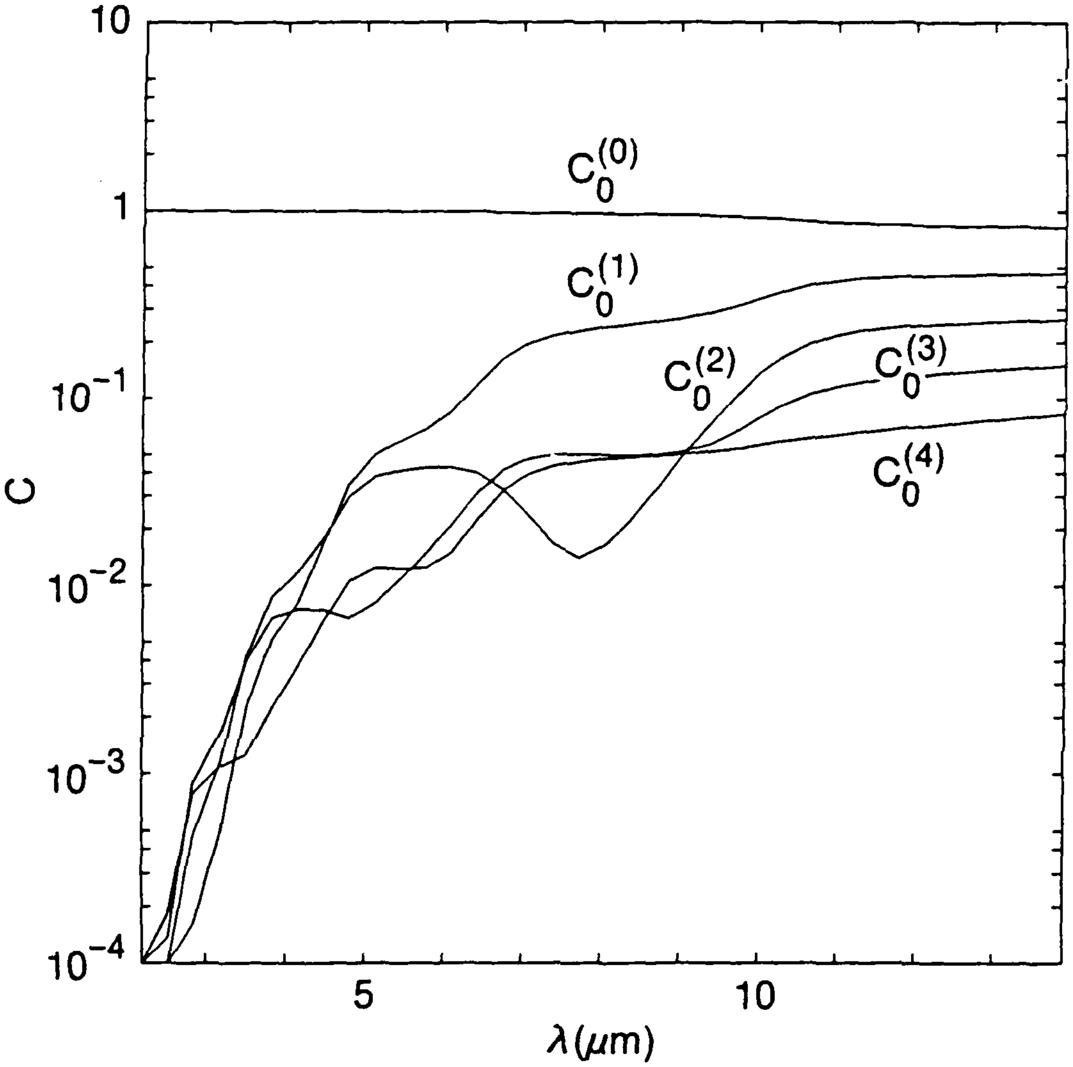

Fig. 5b — Plots of expansion coefficients of the fundamental cavity mode in vacuum modes versus wavelength where the fundamental cavity mode structure has Rayleigh length of $b = L_w/6$ and corresponding mirror curvatures of $R_1 = 523$cm and $R_2 = 389$cm.

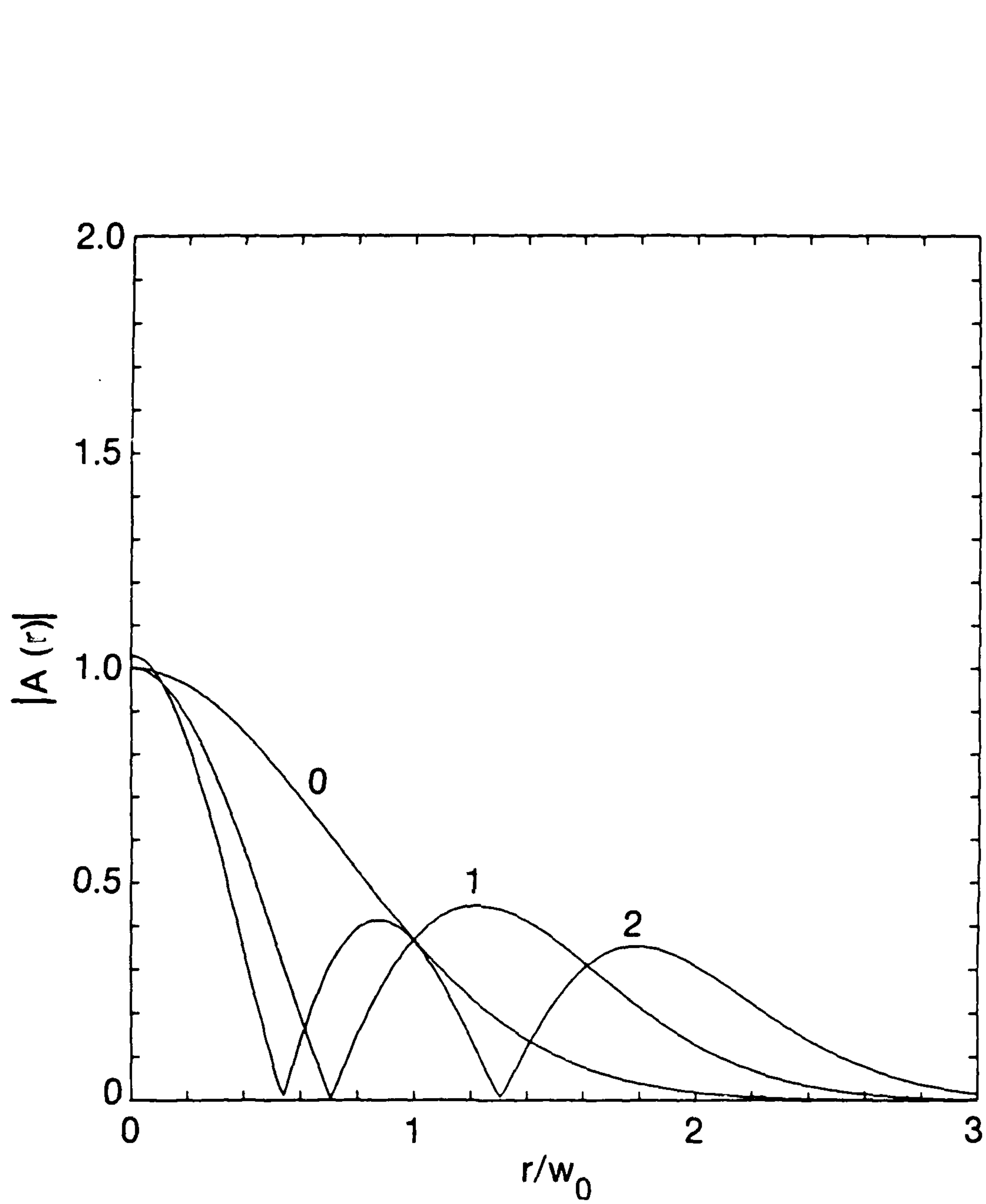

Fig. 5c — Plots of transverse profiles for the first three cavity modes at wavelength 2.2 μm where the fundamental cavity mode structure has Rayleigh length of $b = L_w/6$ and corresponding mirror curvatures of R_1 = 523cm and R_2 = 389cm.

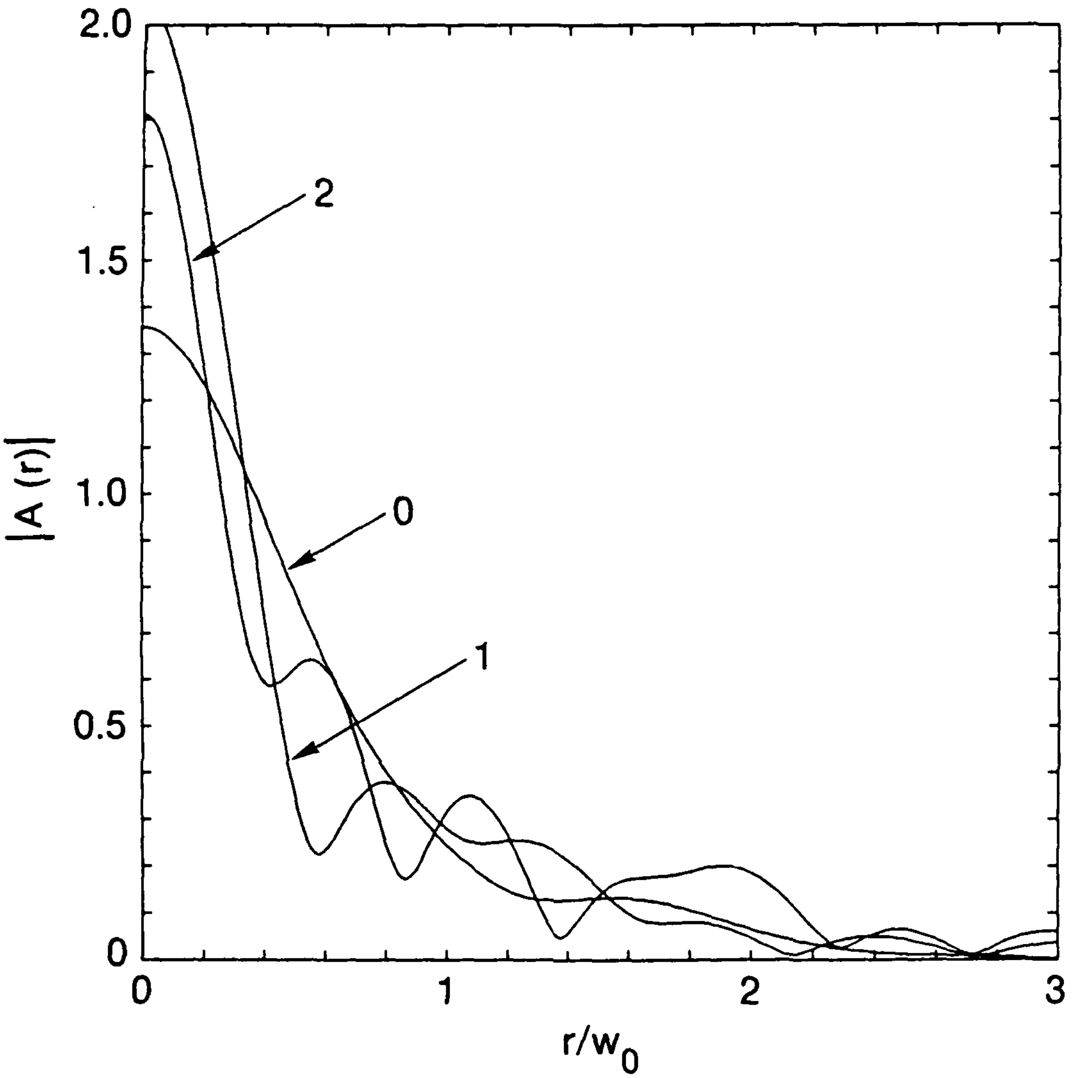

Fig. 5d — Plots of transverse profiles for the first three cavity modes at wavelength 10 μm where the fundamental cavity mode structure has Rayleigh length of $b = L_w/6$ and corresponding mirror curvatures of R_1 = 523cm and R_2 = 389cm.

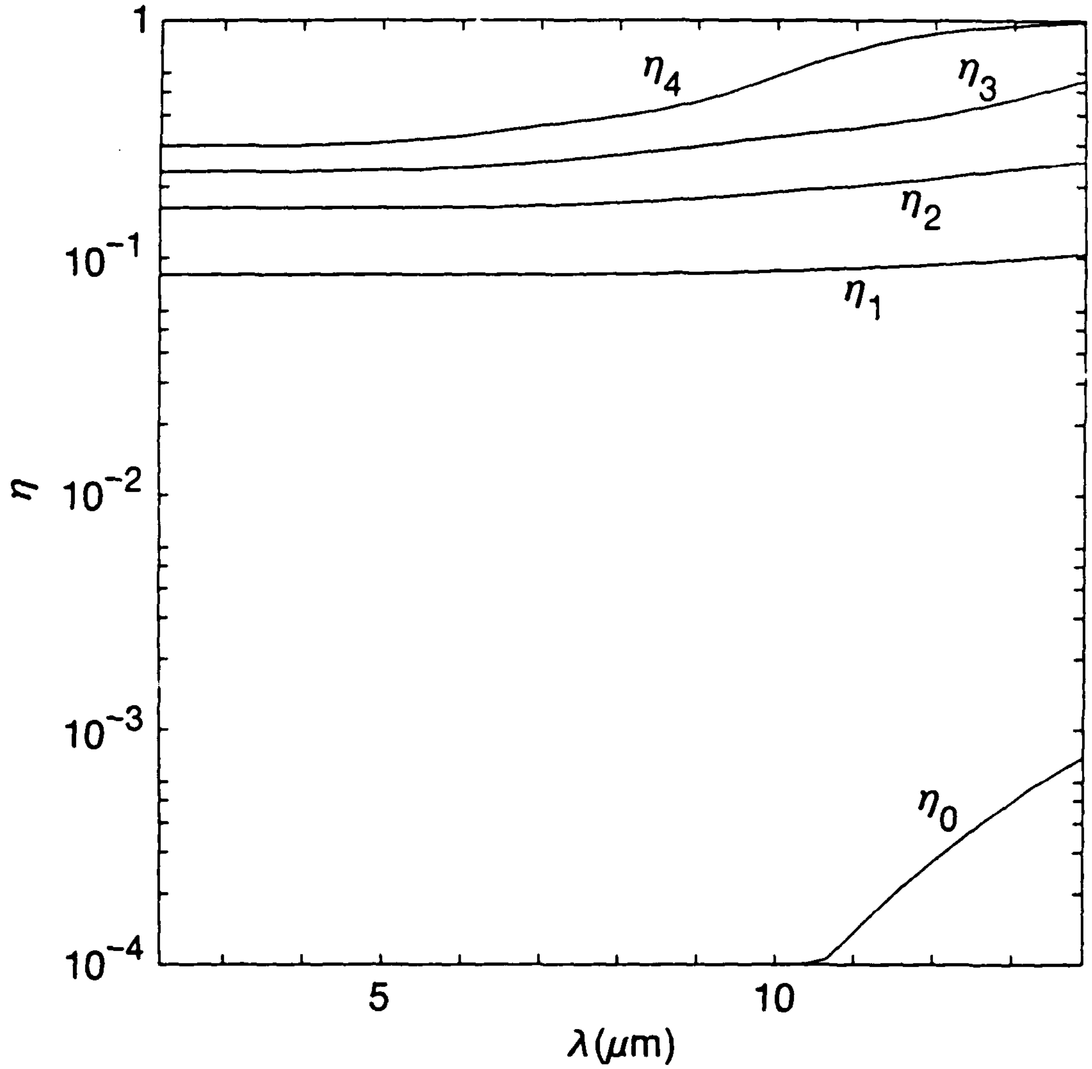

Fig. 6 — Same as in Fig. 2, including the effects of the beam filling factor for small gain.

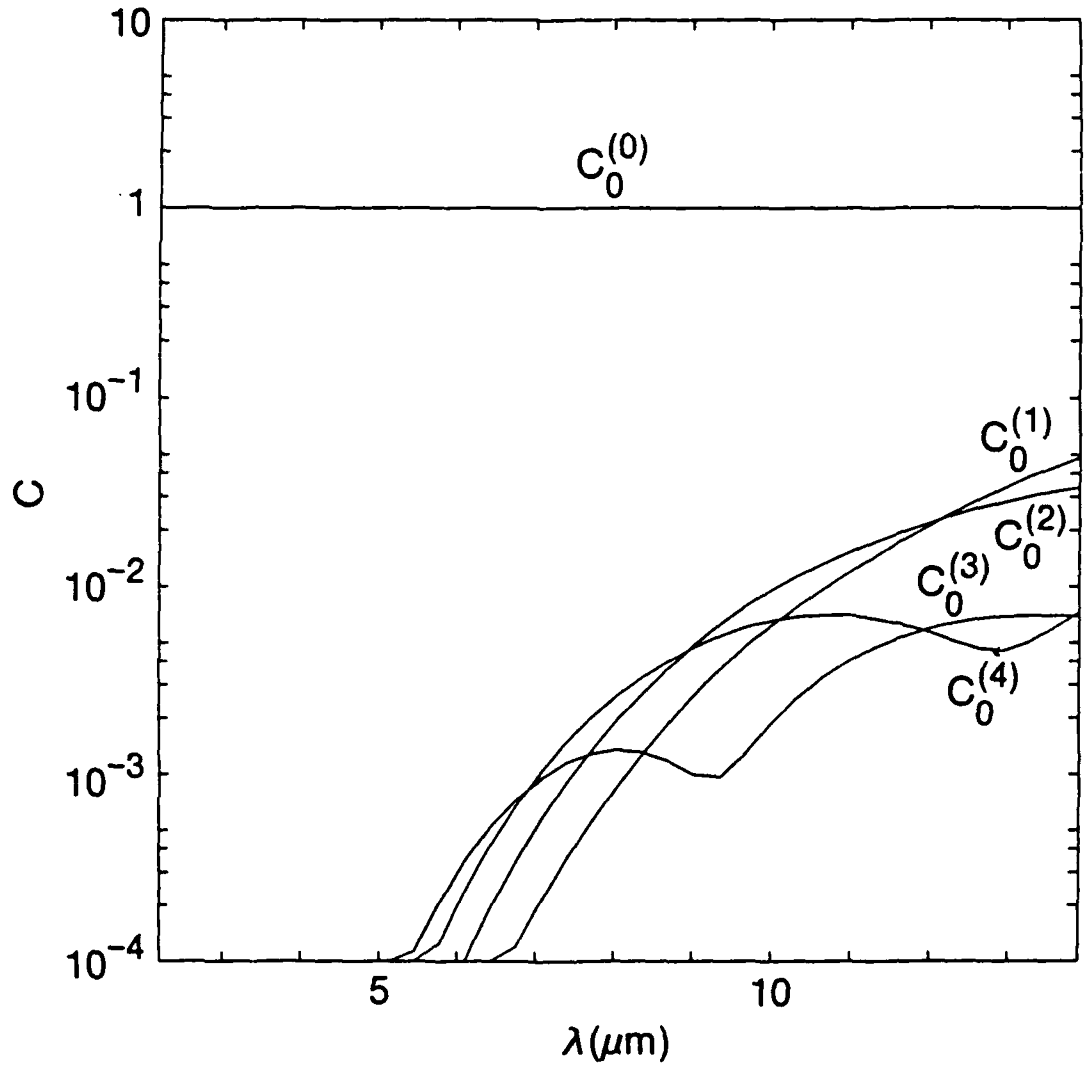

Fig. 7a — Structure of the combined beam-cavity eigenmodes. Same notation as in Fig. 3.

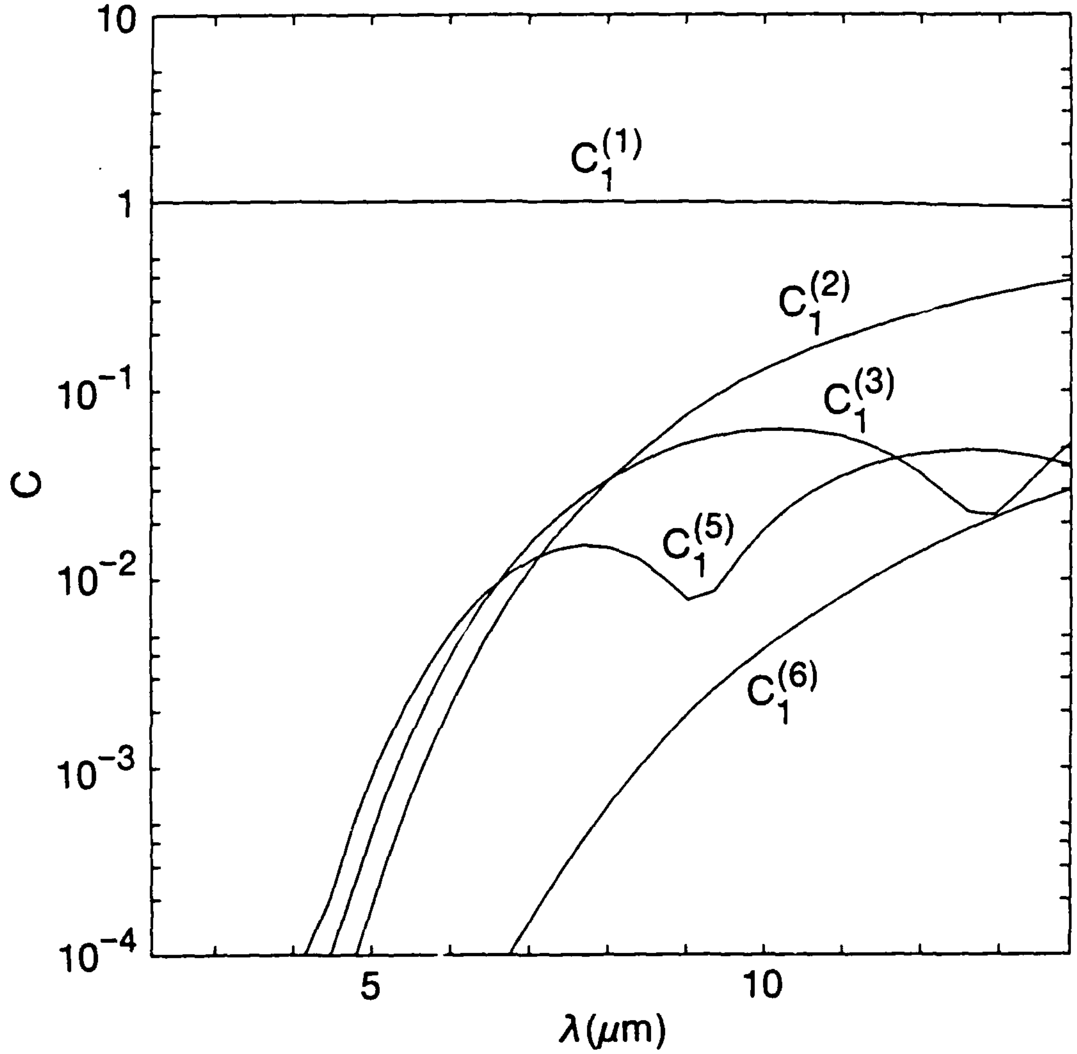

Fig. 7b — Structure of the combined beam-cavity eigenmodes. Same notation as in Fig. 3.

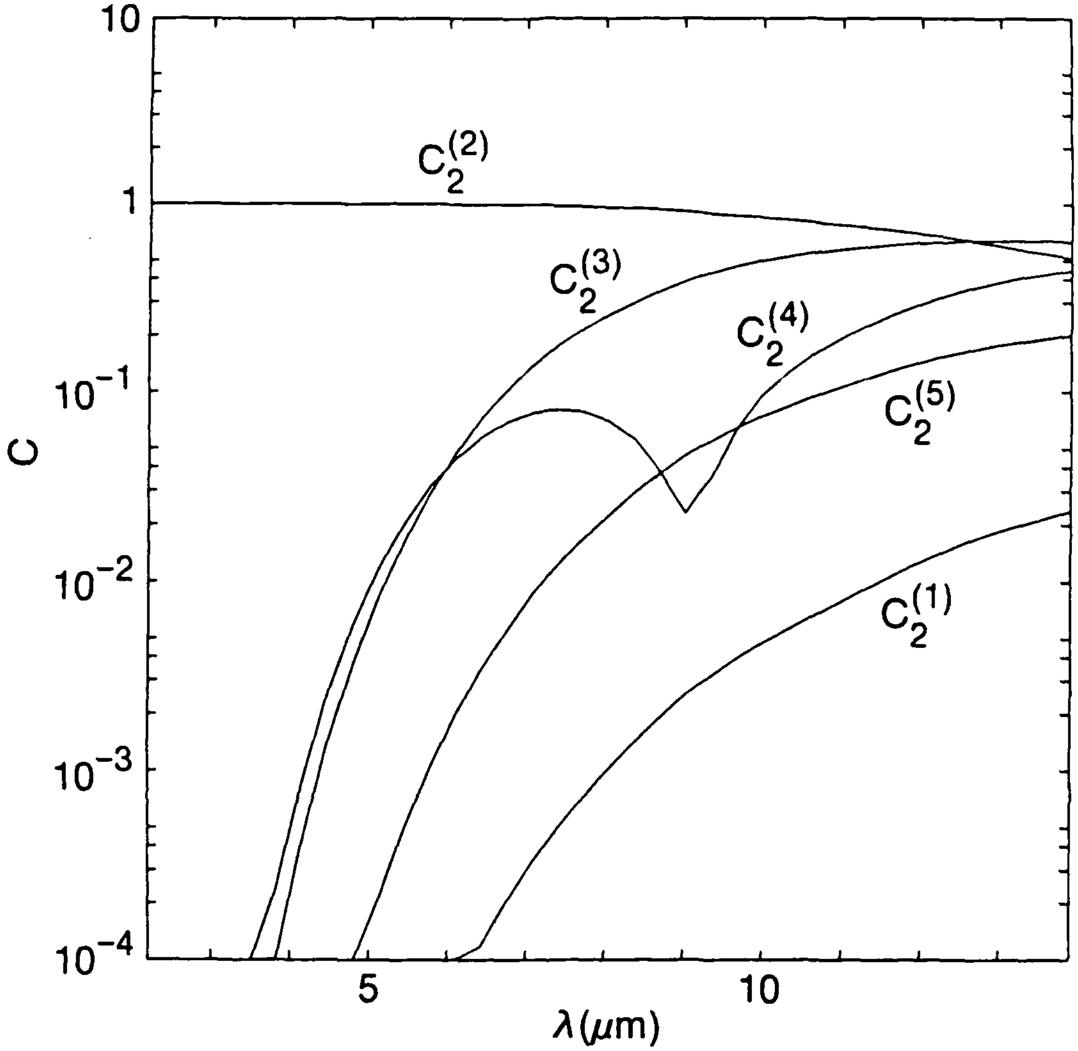

Fig. 7c — Structure of the combined beam-cavity eigenmodes. Same notation as in Fig. 3.

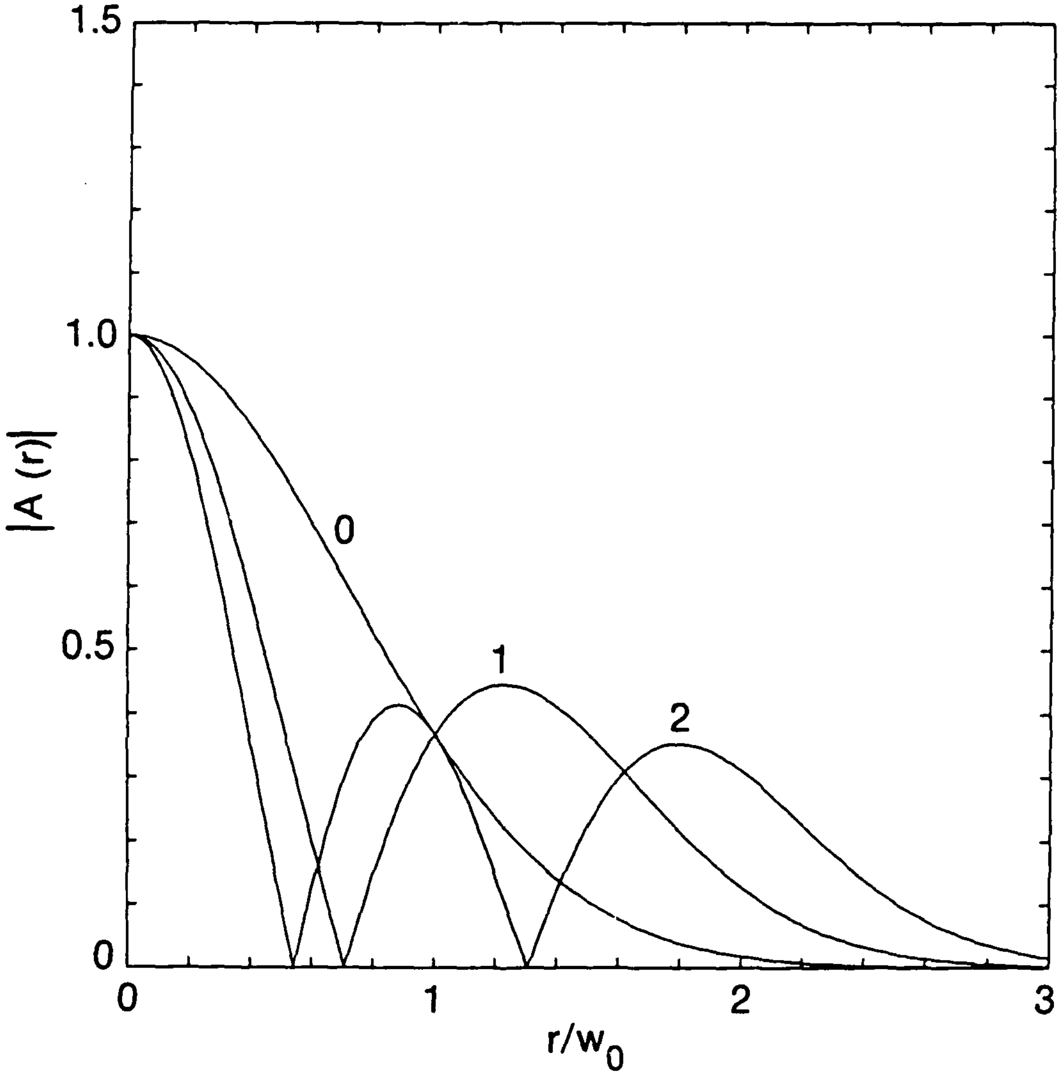

Fig. 8a — Profiles of the first three beam-cavity eigenmodes. Same notation as in Fig. 4.

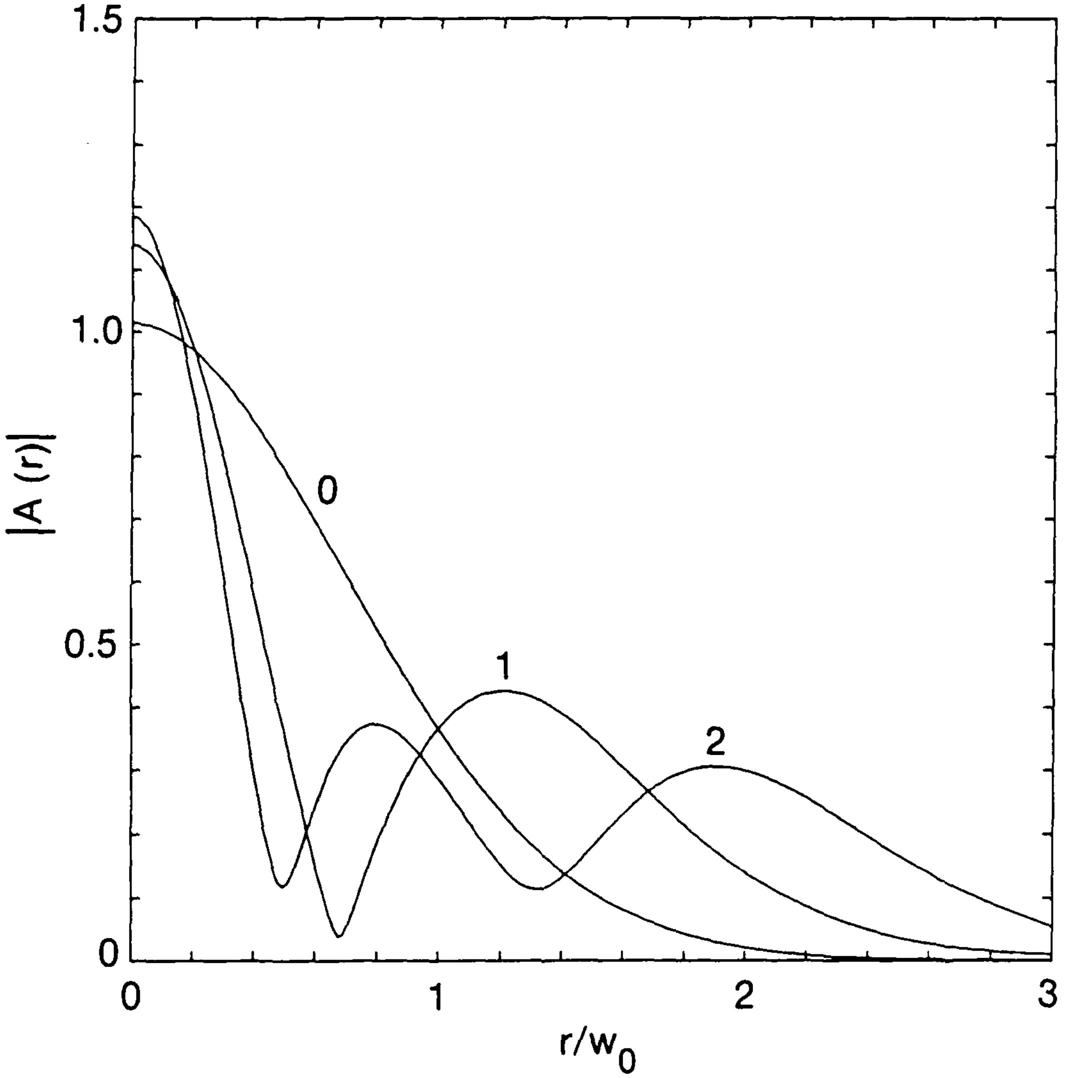

Fig. 8b — Profiles of the first three beam-cavity eigenmodes. Same notation as in Fig. 4.

DISTRIBUTION LIST

Naval Research Laboratory
4555 Overlook Avenue, S.W.
Washington, DC 20375-5000

Attn: Code 1000 - Commanding Officer, CAPT John J. Donegan, Jr.
1001 - Dr. T. Coffey
1005 - Head, Office of Management & Admin.
1005.1-Deputy Head, Office of Management & Admin.
1005.6-Head, Directives Staff
1200 - CAPT R. W. Michaux
1201 - Deputy Head, Command Support Division
1220 - Mr. M. Ferguson
2000 - Director of Technical Services
2604 - NRL Historian
3000 - Director of Business Operations
4000 - Dr. W. R. Ellis
0124 - ONR
4600 - Dr. D. Nagel
4603 - Dr. W. W. Zachary
4700 - Dr. S. Ossakow (26 copies)
4700.1-Dr A. W. Ali
4790 - Dr. P. Sprangle
4790 - Dr. C. A. Kapetanakos
4790 - Dr. J. Mathew
4730 - Dr. R. Elton
4707 - Dr. W. M. Manheimer
4790 - Dr. W. Black
4790 - Dr. A. W. Fliflet
4790 - Dr. S. Gold
4790 - Dr. D. L. Hardesty
4790 - Dr. A. K. Kinkead
4790 - Dr. M. Rhinewine
4770 - Dr. G. Cooperstein
4790 - Dr. C. M. Tang
4790 - Dr. G. Joyce
4790 - Dr. M. Lampe
4790 - Dr. Y. Y. Lau
4790 - Dr. A. Ting
4790 - Dr. E. Esarey
4790 - Dr. J. Krall
4790A- B. Pitcher (copies)
5700 - Dr. L. A. Cosby
5745 - Dr. J. Condon
6840 - Dr. S. Y. Ahn
6840 - Dr. A. Ganguly
6840 - Dr. R. K. Parker
6843 - Dr. R. H. Jackson
6843 - Dr. N. R. Vanderplaats
6843 - Dr. C. M. Armstrong
6875 - Dr. R. Wagner
2628 - Documents (22 copies)
2634 - D. Wilbanks

NOTE: Every name listed on distribution gets one copy except for those where extra copies are noted.

Dr. R. E. Aamodt
Lodestar Research Corp.
2400 Central Ave., P-5
Boulder, CO 80306-4545

Dr. J. Adamski
Boeing Aerospace Company
P.O. Box 3999
Seattle, WA 98124

Dr. T. M. Antonsen
University of Maryland
College Park, MD 20742

Assistant Secretary of the
Air Force (RD&L)
Room 4E856, The Pentagon
Washington, D.C. 20330

Dr. W. A. Barletta
Lawrence Livermore National Lab.
P. O. Box 808
Livermore, CA 94550

Dr. W. Becker
Univ. of New Mexico
Institute for Mod. Opt.
Albuquerque, NM 87131

Dr. Robert Behringer
9342 Balcon Ave.
Northridge, CA 91325

Dr. G. Bekefi
Mass. Institute of Tech.
Room 36-213
Cambridge, MA 02139

Dr. Steven V. Benson
Physics Building
Duke University
Durham, NC 27706

Dr. I. B. Bernstein
Mason Laboratory
Yale University
400 Temple Street
New Haven, CT 06520

Dr. Amitava Bhattacharjee
Columbia University
S. W. Mudd 210
Dept. of Applied Phys.
New York, NY 10027

Dr. Anup Bhowmik
Rockwell International/Rocketdyne Div.
6633 Canoga Avenue, FA-40
Canoga Park, CA 91304

Dr. G. Bourianoff
1901 Rutland Drive
Austin, TX 78758

Dr. Charles Brau
Vanderbilt University
Nashville, TN 37235

Dr. R. Briggs
SSC Laboratory
Stoneridge Office Park
2550 Beckleymeade Ave.
Suite 260
Dallas, TX 75237

Prof. William Case
Dept. of Physics
Grinnell College
Grinnell, IA 50112

Dr. R. Center
Spectra Tech., Inc.
2755 Northup Way
Bellevue, WA 98004

Dr. K. C. Chan
Los Alamos National Laboratory
P. O. Box 1663
Los Alamos, NM 87545

Prof. Frank Chen
School of Eng. & Applied Sciences
Univ. of Calif. at Los Angeles
7731 K Boelter Hall
Los Angeles, CA 90024

Dr. S. Chen
MIT Plasma Fusion Center
NW16-176
Cambridge, MA 01890

Dr. D. P. Chernin
Science Applications Intl. Corp.
1720 Goodridge Drive
McLean, VA 22102

Dr. William Colson
Berkeley Research Assoc.
P. O. Box 241
Berkeley, CA 94701

Dr. Richard Cooper
Los Alamos National Scientific Laboratory
P.O. Box 1663
Los Alamos, NM 87545

Dr. R. A. Cover
Rockwell International/Rocketdyne Div.
6633 Canoga Avenue, FA-38
Canoga Park, CA 91304

Dr. Bruce Danly
MIT
NW16-174
Cambridge, MA 02139

Dr. R. Davidson
Plasma Fusion Center
Mass. Institute of Tech.
Cambridge, MA 02139

Dr. John Dawson
Physics Department
University of California
Los Angeles, CA 90024

Dr. David A. G. Deacon
Deacon Research
Suite 203
900 Welch Road
Palo Alto, CA 94304

Dr. Philip Debenham
Center for Radiation Research
National Bureau of Standards
Gaithersburg, MD 20899

Director
National Security Agency
Fort Meade, MD 20755
ATTN: Dr. Richard Foss, A42
Dr. Thomas Handel, A243
Dr. Robert Madden, R/SA

Director of Research (2 copies)
U. S. Naval Academy
Annapolis, MD 21402

Dr. A. Drobot
Science Applications Intl. Corp.
1710 Goodridge Road
McLean, VA 22102

Dr. Dwight Duston
SDIO/IST
The Pentagon
Washington, DC 20301-7100

Dr. J. A. Edighoffer
TRW, Bldg. R-1
One Space Park
Redondo Beach, CA 90278

Dr. Luis R. Elias
Creol-FEL Research Pavillion
Suite 400
12424 Research Parkway
Orlando, FL 32826

Dr. C. James Elliott
X1-Division, M.S. 531
Los Alamos Natl. Scientific Lab.
P. O. Box 1663
Los Alamos, NM 87545

Dr. Anne-Marie Fauchet
Brookhaven National Laboratories
Associated Universities, Inc.
Upton, L.I., NY 11973

Dr. R. Gajewski
Div. of Advanced Energy Projects
U. S. Dept of Energy
Washington, DC 20545

Dr. J. Gallardo
Brookhaven National Laboratory
Associated Universities, Inc.
Upton, L.I., NY 11973

Dr. B. B. Godfrey,
Chief Scientist
WL/CA
Kirtland AFB, NM 87117-6008

Dr. John C. Goldstein, X-1
Los Alamos Natl. Scientific Lab.
P.O. Box 1663
Los Alamos, NM 87545

Dr. V. L. Granatstein
Dept. of Electrical Engineering
University of Maryland
College Park, MD 20742

Dr. K. Halbach
Lawrence Berkeley Laboratory
University of California, Berkeley
Berkeley, CA 94720

Dr. R. Harvey
Hughes Research Laboratory
3011 Malibu Canyon Road
Malibu, CA 90265

Prof. Herman A Haus
Mass. Institute of Technology
Rm. 36-351
Cambridge, MA 02139

Dr. B. Hui
Defense Advanced Research Projects Agency
1400 Wilson Blvd.
Arlington, VA 22209

Prof. V. Jaccarino
Univ. of Calif. at Santa Barbara
Santa Barbara, CA 93106

Dr. B. Carol Johnson
Ctr. for Radiation Research
National Inst. of Standards and Tech.
Gaithersburg, MD 20899

Dr. Ron Johnson
Ctr. for Radiatiuon Research
Natl. Inst. of Standards and Tech.
Gaithersburg, MD 20899

Dr. Shayne Johnston
Physics Department
Jackson State University
Jackson, MS 39217

Dr. R. A. Jong
Lawrence Livermore National Laboratory
P. O. Box 808/L626
Livermore, CA 94550

Dr. Howard Jory
Varian Associates, Bldg. 1
611 Hansen Way
Palo Alto, CA 94303

Dr. C. Joshi
University of California
Los Angeles, CA 90024

Dr. K. J. Kim, MS-101
Lawrence Berkeley Lab.
Rm. 223, B-80
Berkeley, CA 94720

Dr. Brian Kincaid
Lawrence Berkeley Laboratory
University of California, Berkeley
Berkeley, CA 94720

Prof. N. M. Kroll
Department of Physics
B-019, UCSD
La Jolla, CA 92093

Dr. Thomas Kwan
Los Alamos National Scientific
Laboratory, MS608
P. O. Box 1663
Los Alamos, NM 87545

Dr. J. LaSala
Physics Dept.
U. S. M. A.
West Point, NY 10996

Dr. Michael Lavan
U.S. Army Strategic Def. Command
ATTN: Code CSSD-H-D
P. O. Box 1500
Huntsville, AL 35807-3801

Dr. B. Levush
Dept. of Physics & Astronomy
University of Maryland
College Park, MD 20742

Dr. Anthony T. Lin
Dept. of Physics
University of California
Los Angeles, CA 90024

Dr. Chuan S. Liu
Dept. of Physics & Astronomy
University of Maryland
College Park, MD 20742

Dr. A. Luccio
Brookhaven National Laboratory
Accelerator Dept.
Upton, NY 11973

Prof. J.M.J. Madey
117 Physics Bldg.
Duke University
Durham, NC 27706

Dr. R. Mako
205 South Whiting Street
Alexandria, VA 22304

Dr. Joseph Mangano
Science Research Laboratory
1600 Wilson Blvd.
Suite 1200
Arlington, VA 22209

Dr. Siva A. Mani
Science Applications Intl. Corp.
1040 Waltham Street
Lexington, MA 02173-8027

Dr. T. C. Marshall
Applied Physics Department
Columbia University
New York, NY 10027

Dr. Xavier K. Maruyama
Dept. of Physics
Naval Postgraduate School
Monterey, CA 93943

Dr. B. McVey
Los Alamos National Laboratory
P. O. Box 1663
Los Alamos, NM 87545

Dr. David Merritt
Space & Naval Warfare Command
Attn: PMW 145A
Washington, DC 20363-5100

Dr. A. Mondelli
Science Applications Intl. Corp.
1710 Goodridge Drive
P.O. Box 1303
McLean, VA 22101

Dr. Mel Month
Brookhaven National Laboratories
Associated Universities, Inc.
Upton, L.I., NY 11973

Dr. Gerald T. Moore
University of New Mexico
Albuquerque, NM 87131

Dr. Philip Morton
Stanford Linear Accelerator Center
P.O. Box 4349
Stanford, CA 94305

Prof. J. Nation
224 Phillips Hall
School of Elec. Eng.
Cornell University
Ithaca, NY 14850

Dr. George Neil
TRW
One Space Park
Redondo Beach, CA 90278

Dr. Kelvin Neil
Lawrence Livermore National Lab.
Code L-321, P.O. Box 808
Livermore, CA 94550

Dr. Brian Newnam
MSJ 564
Los Alamos National Scientific Lab.
P.O. Box 1663
Los Alamos, NM 87545

Dr. T. Orzechowski
L-436
Lawrence Livermore National Lab.
P. O. Box 808
Livermore, CA 94550

Prof. E. Ott
Department of Physics
University of Maryland
College Park, MD 20742

OUSDRE (R&AT)
Room 3D1067, The Pentagon
Washington, D.C. 20301

Dr. Robert B. Palmer
Brookhaven National Laboratories
Associated Universities, Inc.
Upton, L.I., NY 11973

Dr. J. Palmer
Hughes Research Laboratory
Malibu, CA 90265

Dr. Richard H. Pantell
Stanford University
Stanford, CA 94305

Dr. Dennis Papadopoulos
Astronomy Department
University of Maryland
College Park, Md. 20742

Dr. John A. Pasour
Mission Research Laboratory
8560 Cinderbed Road
Suite 700
Newington, VA 22122

Dr. C. K. N. Patel
Bell Laboratories
Murray Hill, NJ 07974

Dr. Claudio Pellegrini
Brookhaven National Laboratory
Associated Universities, Inc.
Upton, L.I., NY 11973

Dr. S. Penner
Center for Radiation Research
Natl. Inst. of Standards and Tech.
Gaithersburg, MD 20899

Dr. M. Piestrup
Adelphi Technology
13800 Skyline Blvd. No. 2
Woodside, CA 94062

Dr. D. J. Pistoresi
Boeing Aerospace Company
P. O. Box 3999
Seattle, WA 98124-2499

Major E. W. Pogue
SDIO
The Pentagon, T-DE Rm. 1E180
Washington, DC 20301-7100

Major Donald Ponikvar
U. S. Army SDC
P. O. Box 15280
Arlington, VA 22245-0280

Dr. Donald Prosnitz
Lawrence Livermore National Lab.
Box 5511 L-626
Livermore, CA 94550

Dr. D. C. Quimby
Spectra Technology
2755 Northup Way
Bellevue, WA 98004

Dr. G. Ramian
Quantum Institute
University of California
Santa Barbara, CA 93106

Dr. M. Reiser
University of Maryland
Department of Physics
College Park, MD 20742

Dr. S. Ride
Arms Control
Stanford University
Stanford, CA 94305

Dr. C. W. Roberson
Office of Naval Research
Code 112S
800 N. Quincy Street
Arlington, VA 22217

Dr. K. Robinson
Spectra Technology
2755 Northup Way
Bellevue, WA 98004

Dr. Marshall N. Rosenbluth
Dept. of Physics
B-019
Univ. of Calif., San Diego
LaJolla, CA 92093

Dr. J. B. Rosenzweig
The Inst. for Accelerator Physics
Department of Physics
University of Wisconsin-Madison
Madison, WI 53706

Dr. N. Rostoker
Department of Physics
University of California at Irvine
Irvine, CA 92717

Dr. A. Saxman
Los Alamos National Scientific Lab.
P. O. Box 1663, MSE523
Los Alamos, NM 87545

Dr. E. T. Scharlemann
L626
Lawrence Livermore National Laboratory
P. O. Box 808
Livermore, CA 94550

Prof. S. P. Schlesinger
Dept. of Electrical Engineering
Columbia University
New York, NY 10027

Dr. Howard Schlossberg
AFOSR
Bolling AFB
Washington, D.C. 20332

Dr. George Schmidt
Stevens Institute of Technology
Physics Department
Hoboken, NJ 07030

Dr. M. J. Schmitt
Los Alamos National Laboratory
P. O. Box 1663
Los Alamos, NM 87545

Dr. H. Schwettmann
Phys. Dept. & High Energy
Physics Laboratory
Stanford University
Stanford, CA 94305

Dr. Marlan O. Scully
Dept. of Physics & Astronomy
Univ. of New Mexico
800 Yale Blvd. NE
Albuquerque, NM 87131

Dr. S. B. Segall
KMS Fusion
3941 Research Park Dr.
P.O. Box 1567
Ann Arbor, MI 48106

Prof. P. Serafim
Northeastern University
Boston, MA 02115

Dr. A. M. Sessler
Lawrence Berkeley Laboratory
University of California
1 Cyclotron Road
Berkeley, CA 94720

Dr. W. Sharp
L-626
Lawrence Livermore National Laboratory
P. O. Box 808
Livermore, CA 94550

Dr. Earl D. Shaw
Bell Laboratories
600 Mountain Avenue
Murray Hill, NJ 07974

Dr. R. L. Sheffield
Los Alamos National Laboratory
P.O. Box 1663
Los Alamos, NM 87545

Dr. D. Shoffstall
Boeing Aerospace Company
P.O. Box 3999
Seattle, WA 98124

Dr. Jack Slater
Spectra Technology
2755 Northup Way
Bellevue, WA 98004

Dr. Todd Smith
Hansen Labs
Stanford University
Stanford, CA 94305

Dr. R. Sudan
Lab. of Plasma Studies
Cornell University
Ithaca, NY 14850

Dr. David F. Sutter
ER 224, GTN
Department of Energy
Washington, D.C. 20545

Dr. T. Tajima
Institute for Fusion Studies
University of Texas at Austin
Austin, TX 78712

Dr. R. Temkin
Mass. Institute of Technology
Plasma Fusion Center
Cambridge, MA 02139

Dr. L. Thode
Los Alamos National Laboratory
P. O. Box 1663
Los Alamos, NM 87545

Dr. Norman H. Tolk
Physics Department
Vanderbilt University
Nashville, TN 37240

Dr. Kang Tsang
Science Applications Intl. Corp.
1710 Goodridge Dr.
McLean, VA 22102

Dr. H. S. Uhm
Naval Surface Warfare Center
White Oak Lab.
Silver Spring, MD 20903-5000

Under Secretary of Defense (R&D)
Office of the Secretary of Defense
Room 3E1006, The Pentagon
Washington, D.C. 20301

Dr. John E. Walsh
Wilder Laboratory
Department of Physics (HB 6127)
Dartmouth College
Hanover NH 03755

Dr. Jiunn-Ming Wang
Brookhaven National Laboratories
Associated Universities, Inc.
Upton, L.I., NY 11973

Dr. Roger W. Warren
Los Alamos National Scientific Lab.
P.O. Box 1663
Los Alamos, NM 87545

Dr. J. Watson
Los Alamos National Laboratory
P. O. Box 1663
Los Alamos, NM 87545

Dr. Mark Wilson
Natl. Inst. of Standards and Tech.
Bldg. 245, Rm. B-119
Gaithersburg, MD 20899

Dr. J. Wurtele
M.I.T.
NW 16-234
Plasma Fusion Center
Cambridge, MA 02139

Dr. Ming Xie
Dept. of Physics
Stanford University
Stanford, CA 94305

Dr. Yi-Ton Yan
Stanford Linear Accelerator Center
P. O. 4349
Stanford, CA 94305

Dr. Simon S. Yu
Lawrence Livermore National Laboratory
P. O. Box 808
Livermore, CA 94550